The Effects of Placental Mesenchymal Stem Cells Labelled With Ultrasmall Superparamagnetic Iron Oxides on the Growth of Colorectal Cancer (CRC) Cells

Fang Wang
Ningxia Medical University
Hua He
General Hospital of Ningxia medical university
Yao Xiong
Ningxia Medical College: Ningxia Medical University
Jie-ting HU
Ningxia Medical College: Ningxia Medical University
Yu-lin Guo (guoyulin66@126.com)
General Hospital of Ningxia medical university

Research

Keywords: Colorectal cancer, Placental mesenchymal stem cells (PMSCs), Ultrasmall superparamagnetic iron oxides (USPIOs), Magnetic resonance imaging

Posted Date: December 8th, 2020

DOI: https://doi.org/10.21203/rs.3.rs-120624/v1

Abstract

Objective: To investigate the effects of human placental mesenchymal stem cells (PMSCs) labelled with ultrasmall superparamagnetic iron oxides (USPIOs) on the growth of colorectal cancer (CRC) cells and the feasibility of 3.0T MR in vivo tracer.

Methods: PMSCs were labelled with USPIOs, the labeling efficiency was determined by Prussian blue-stained, and their biological characteristics were identified. A subcutaneous CRC HT-29 xenograft model in immunodeficient mice was established, and we attempted to consider the group was injected with labelled MSCs as experimental group. The growth and MR signal changes of xenograft tumors of nude mice was assessed, then, plot growth curve and analyzed the MR image quality in different sequences, obtained the pathological results after scan.

Results: 1. USPIOs-labelled PMSCs had no significant influence on biological characteristics, such as cell viability, proliferation ability, and apoptosis rate ($P > 0.05$). 2. The regions with low signal value could be observed in the experimental group on the first day on the MR. On the 7th day, the regions with low signal value were narrowed, and in some tumors showed poor clarity, whereas the signal values did not significantly change. The trend of growth of tumors in mice in the experimental group before injection of PMSCs was similar to that of the control group, while growth rate of tumor in the experimental group on day 5 after injection of PMSCs was slightly lower than that in the control group, and the volume of tumor on day 14 was noticeably smaller than that in the control group. There was no significant difference in the positive expression rates of CD31, CD34, and Ki67 between the two groups ($P > 0.05$). 3. The tracing ability of T2* mapping sequences for USPIOs-labelled cells was superior than T2WI and T2 mapping sequences.

Conclusion: USPIOs-labelled PMSCs had high labeling efficiency, while cell viability, proliferation ability, and apoptotic rate were not markedly influenced. labelled cells injected into CRC transplanted tumors were studied for a long period of time, and only a certain inhibitory effect on growth of tumor volume was noted, while no meaningful influence on tumor proliferation and angiogenesis was found.

Background

Colorectal cancer (CRC) is one of the most common malignant tumors worldwide. In 2018, there were globally 1.804 million new cases, and its morbidity and mortality rank the third in malignant tumors[1, 2]. CRC lacks specific clinical symptoms in the early stage, and the majority of patients are in the middle and advanced stages at the time of consultation, with poor prognosis[3]. Thus, effective intervention and treatment are highly essential for CRC.

The necessary nutrients to maintain tumor growth depend on tumor neovascularization, therefore, the tumor microenvironment has reached steady-state, and "normalization" of tumor blood vessels has become a new strategy for tumor treatment[4–7]. Because placental mesenchymal stem cells (PMSCs) have weak immunogenicity, tumorigenicity, and biological characteristics that are easy to introduce and

express foreign genes [8, 9], they showed great application prospects as anti-tumor gene-loaded cells in recent years [10, 11]. Some studies reported that MSCs have remarkable influences on tumor neovascularization, and they can promote tumor growth by promoting the expression of vascular endothelial growth factor (VEGF), participating in formation of tumor stroma, enhancing tumor cell activity, or inhibiting tumor growth and metastasis through mechanisms, such as targeted chemotaxis and differentiation.

The possible mechanism of tumor inhibition via MSCs was attributed to the soluble factors secreted by these cells, including Dickkopf-related protein 1 (DKK1), playing a role in the inhibition of Wnt signaling pathways in tumor cells [12–14]. While magnetic resonance imaging (MRI) is routinely used to obtain specific and high-resolution images of cancer tissues, developing clinically feasible targeted MRI contrast agents for MR molecular imaging of the biomarkers expressed on cancer cell surface is challenging, due to the low sensitivity of MRI and low concentration of the biomarkers. A research demonstrated the use of ultrasmall superparamagnetic iron oxides (USPIOs) extensively as blood pool MRI contrast agents[15]. Besides, high-resolution MRI with USPIOs showed promising results in detecting smaller lymph nose metastases [16, 17].

Hence, in the present study, we established a subcutaneous CRC HT-29 xenograft model in immunodeficient mice, and used USPIO to label PMSCs, then USPIOs were injected into transplanted tumors of mice, explored MRI characteristics and quality of different MR sequences. Combined with pathological results, the role of PMSCs in tumor cell growth and angiogenesis was analyzed,in order to provide a more reliable basis for targeted therapy of CRC.

Materials And Methods

Cultivation of PMSCs

Human PMSCs were donated by the Stem Cell Research Institute of the General Hospital of Ningxia Medical University (Yinchuan, China). PMSCs were cultured and concentration was adjusted to 3×10^6 cells/mL, 100 uL cell suspension was added to Eppendorf (EP) tube, and then, 2 uL primary antibodies (CD29, CD105, CD73, CD11b, CD14, CD45, and IgG1) was added, incubated at 4 ℃ for 30 min, centrifuged, washed, and the supernatant was removed. Afterwards, 2uL FITC-conjugated secondary antibody was added to incubate in an ice box in the dark for 30 min, which then centrifuged, washed with phosphate-buffered saline (PBS), and finally the positive expression rate of cell surface markers was detected.

USPIOs-labelled PMSCs

Prepared cells were seeded into a six-well plate with a density of 2×10^4 cells/ml. After the cells adhere to the wall, add 1.5 mL culture medium, and then incubated. Next, USPIOs and poly-L-lysine (PLL) were

mixed at a ratio of 1:0.03, placed in a vortex mixer at 2200 r/min, and shaken for 30 min to form PLL-USPIO complex, then add to cultere medium at a final concentration of 10uL/mL. After incubation for 24 h, it was fixed with 4% paraformaldehyde, and stained with Perls' Prussian blue. The number of Prussian blue-stained and unstained cells were counted using hemocytometer (× 100) under an inverted microscope and labeling efficiency was determined by percentage of Prussian blue-stained positive cells over total cells.

Comparing biological characteristics of PMSCs

The Trypan Blue dye exclusion test: This test was carried out to determine the number of viable cells present in a cell suspension. Take an equal amount of PMSCs suspension and 0.4% Trypan blue solution to mix and count, due to incomplete cell membrane, dead cells can be stained blue and living cells are not stained. Besides, cell counting kit-8 (CCK-8) was used to assess cell proliferation; for this purpose, 2×10^3 PMSCs were seeded into 96-well plates, and we attempted to consider the labelled cells as experimental group, the unlabelled cells as control group, and the medium without cells was Blank group (there were 5 duplicate wells in each group). On the 1st, 3rd, 5th, and 7th days after labeling, 10 uL CCK-8 solution was added to 100 uL complete medium, incubated for 2 h to detect optical density (OD) value of each well at a wavelength of 450 nm, then, the OD value of different groups were compared, and the cell proliferation curve was plotted. Additionally, Annexin V-FITC/PI cell apoptosis detection kit was utilized to detect the rate of apoptosis rate; to this end, labelled and unlabelled PMSCs were collected, and the cell density was adjusted to 1×10^5 cells/ml. Furthermore, 500 μL of 1 × Annexin V Binding Buffer was added to re-suspend the cells. Next, the cells were gently vortexed, and incubated at room temperature for 15 min in the dark.

Establishment of animal models

Herein, 20 healthy female BALB/c nude mice (body weight, 18–22 g; age, 4–6 week-old) were tested, and fed at Experimental Animal Center of Ningxia Medical University (Yinchuan, China). Moreover, 20 nude mice were randomly divided into two groups (n = 10 mice for each group). The concentration of HT-29 cells was adjusted to 10^7 cells/ml, and subcutaneously inoculated into the right groin of nude mice. The experiment was performed on the day 14 when the tumor diameter was about 5 mm. In the experimental group, 5×10^6 cells/mL of USPIOs-labelled PMSCs were injected into tumor-bearing mice, while no injection was undertaken in the control group. The growth of xenograft tumors of nude mice was assessed, then, diameter of each transplanted tumor was measured every 3–4 days, and the growth curve was plotted to calculate the volume of tumor.

MRI scan in vivo

4% isoflurane to induce anesthesia, when the mice under deep anesthesia adjusted the concentration to 1.5% for continuing anesthesia. Scanning parameters: T2WI fast spin echo sequence TR 2000 ms, TE 140 ms, echo chain length 15, flip angle = 150°, FOV 35 mm × 35 mm, acquisition matrix 176 × 176; T2 mapping sequence: TR 2000 ms, TE n * 13 ms, six echoes of 13, 26, 39, 52, 65, 78 ms, flip angle = 90°, FOV 50 mm × 50 mm, acquisition matrix 124 × 124; T2 * mapping sequence: TR 28 ms, TE n * 3 ms are six echoes of 3, 8, 12, 16, 20, 24 ms, flip angle = 20°, FOV 30 mm × 30 mm, matrix 100 × 96. Transverse scanning, layer thickness 2 mm, layer spacing 0.2 mm,and scanned before the PMSCs injection, on the 1st, 2nd, 3rd, 7th, 10th, and 14th days, analyzed the signal change rates (△SI, △T2, △T2 *) and plotted time signal value curve, compared the SNR, CNR and C values of each sequence. △SI = [(SIlabeled-SItumor) / SItumor] × 100%, △T2 = (T2labeled-T2tumor) / T2tumor] × 100%, △T2 * = (T2 * labeled-T2 * tumor) / T2 * tumor] × 100%, SNR = SItumor / SDnoise, CNR = SItumor-SIlabeled / SDnoise, C = SItumor / SIlabeled (SIlabeled, SItumoris is the signal strength of labeled cells and tumor, SDnoise is the standard deviation of background signal strength). Avoided bleeding and necrosis to measure tumor tissue, and choosed the contralateral thigh's largest section to measure muscle, The region of interest(ROI) size of tumor and image background was 3 cm^2 and the labeled area was 0.5 cm^2, three ROIs were selected and averaged.

Pathological assessment

Herein, 2 mice were selected from both the experimental group and the control group respectively to be sacrificed on the 2nd day of PMSCs injection for Perls' Prussian blue staining, and the remaining mice were sacrificed after MRI on the 14th day of PMSCs injection. The inhibition rate of tumor growth was calculated using the following formula: inhibition rate (%) = (mean tumor weight in control group – mean tumor weight in experimental group)/ mean tumor weight in control group × 100%. Moreover, hematoxylin and eosin (H&E), Perls' Prussian blue,and CD31, CD34, and ki67 staining methods were performed, and microvascular density (MVD) was calculated by modifying the Weidner method.

Statistical analysis

The data were statistically analyzed by SPSS 23.0 software (IBM, Armonk, NY, USA), and all experimental data were expressed as mean ± standard deviation (x ± s). The rates of survival, apoptosis, proliferation, and tumor inhibition of labelled and unlabelled cells were compared by the independent t-test. The volume of transplanted tumors was analyzed by repeated measures analysis of variance (ANOVA). The values of signal-to-noise ratio (SNR) and contrast-to-noise ratio (CNR) for each sequence were compared by ANOVA. $P < 0.05$ was considered statistically significant.

Results

Identification of PMSCs

After inoculation of PMSCs for 24 h, the cells became flat and irregular, which could be observed under a microscope. Results of flow cytometry analysis showed that the expression rates of CD29, CD73, and CD105, were 99.4%, 98.5%, and 96.0%, respectively, while CD11b, CD14, and CD44 were hardly expressed (Fig. 1). The Prussian-blue-stained particles were found in the cytoplasm of magnetized labelled cells, which could be observed under a fluorescence microscope, and the labeling rate > 95% (Fig. 2).

Cell biological characteristics

Cell viability: The survival rate of the cells in the unlabelled group and the labelled group was (95.50 ± 0.50)% and (94.69 ± 0.11)% after 24 h. The survival rate was compared between the two groups (t = -0.81, P = 0.58), indicating that the USPIOs-labelled PMSCs did not significantly affect cell viability. Cell proliferation ability: The trend of the cells labelled with USPIOs from day 1 to day 7 was similar to that of unlabelled cells, and the optical density (OD) value increased over time. P-values compared on days 1, 3, and 5 in the labelled group and the control group were 0.83, 0.06, and 0.22, respectively, indicating that USPIOs-labelled PMSCs had no significant influence on the cell proliferation within a certain period of time (Fig. 3). Apoptosis rate: It was revealed that apoptosis rate was significantly different between labelled group and unlabelled group (t = 15.40, P = 0.21), indicating that the USPIOs-labelled PMSCs also had no remarkable influence on the apoptosis rate (Fig. 4).

Growth of transplanted tumors

The incubation period of HT-29 cells were transplanted via subcutaneous injection was about 5 days, cyclical mounds with diameter of about 3 mm were noted in each groin of tumor-bearing mice, and there were subcutaneous nodules with diameter of about 4–5 mm after 2 weeks. The mass of a nodule with a clear boundary of about 6–7 mm was increased after 3 weeks, and the tumor diameter was about 8–10 mm after 4 weeks. As shown in Fig. 5, the trend of growth of tumors in mice in the experimental group before injection of PMSCs was similar to that of the control group, while growth rate of tumor in the experimental group on day 5 after injection of PMSCs was slightly lower than that in the control group, and the volume of tumor on day 14 was noticeably smaller than that in the control group. However, the volume of tumor was notably different between the two groups (F = 0.001, P = 0.972), while the weight of tumor was not statistically different after 14 days (t = 0.065, P = 0.949). The tumor inhibition rate could not be calculated, indicating that the injection of PMSCs had no significant effect on volume and weight of tumors compared with the control group.

Changes of MR signal

The T2WI, T2 mapping, and T2 * mapping sequences of the transplanted tumor all showed high signals. In the experimental group (the 1st day), T2WI, T2 mapping, and T2 * mapping sequences showed bar-shaped low-signal regions, and T2 and T2 * values were significantly lower, while T2 * value markedly

changed in tumor tissues; the signal value was the lowest on the 2nd day after injection of PMSCs; on the 3rd day, the signal value of the USPIOs-labelled PMSCs gradually increased, and the signal value in the tumor tissue was the lowest; on the 7th day, the region with low-signal was unclear in some tumors, and the signal values of tumor tissues and USPIOs-labelled PMSCs did not noticeably change; on the 10th day, the signal value of the tumor significantly increased, and the change of the signal value gradually decreased over time. The change of intensity had no obvious influence on the experiment, in which the transplanted tumor in the control group showed a high signal and the volume of the transplanted tumor increased over time. On the 14th day, a large area of high signal necrosis appeared in the both groups (Figs. 6–8).

Quality of MR images

In the 3.0T MR, T2 mapping and T2 * mapping sequences showed different TE value image quality, in which TE value increased with significantly reduction of SNR, and the value of CNR slightly increased (Fig. 9). Comparison of SNR value for each sequence revealed the following consequences: P = 0.000 for T2WI vs. T2 mapping, P = 0.037 for T2WI vs. T2 * mapping, P = 0.045 for T2 mapping vs. T2 * mapping, and the SNR of T2 * mapping sequence for USPIOs-labelled PMSCs was higher than that in T2WI and T2 mapping sequence. Comparison of CNR value for each sequence unveiled the following outcomes: P = 1.000 for T2WI vs. T2 mapping, P = 0.015 for T2WI vs. T2 * mapping, P = 0.000 for T2 mapping vs. T2 * mapping, and the contrast of T2 * mapping sequences of USPIOs-labelled PMSCs was greater than that of T2WI and T2 mapping sequences (Table 1).

Table 1
Comparison of Image Quality by Sequence

Evaluating indicator	T2WI	T2mapping	T2*mapping	*F* value	*P* value
SNR	44.078 ± 19.704	88.085 ± 21.007	66.578 ± 6.347	10.020	0.002
CNR	20.480 ± 12.967	20.785 ± 1.529	44.797 ± 1.021	2.428	0.000
C	1.895 ± 0.426	1.342 ± 0.128	3.242 ± 0.756	14.363	0.001

Pathological findings

HE staining showed that the tumor was a poorly differentiated adenocarcinoma with larger cancer cells, unclear cytoplasmic boundaries, thickened tumor stroma, thin-walled blood vessels, and diverse nucleus morphology. It was disclosed that on the next day of injection of PMSCs, the Prussian-blue-stained particles could be observed in the edge area of tumor tissue. Besides, positively expressed CD31 and CD34 cells were found in both the experimental group and the control group, and the neovascularization was rich and distributed in form of brown strips. The MVD in the experimental group and control group

was 65 ± 15.7 and (62 ± 14.3), respectively. Comparison of positively expressed CD31 cells between the experimental group and the control group showed t = 0.245 (P = 0.819), while that was t = 0.270 (P = 0.800) for positively expressed CD34 cells. Besides, the MVD was consistent in the two microvascular endothelial markers (P > 0.05). The positive rate of ki67 was greater than 50%, there was no meaningful influence on tumor proliferation between the two groups,too. (Fig. 10)

Discussion

The efficient application of stem cells for the treatment of neurodegenerative diseases requires safe cell tracking to follow stem cell fate over time in the host after transplantation. It is noteworthy that T2 mapping and T2 * mapping use echo-signal curve fitting to form pseudo-color maps to quantify iron particles in tissues, which can indirectly reflect the iron concentration in the tissues. Therefore, T2WI, T2 mapping, and T2 * mapping sequences are widely used worldwide [18]. The present research revealed that the intensity of MR signal didn't significantly change over time, and thus, cannot be used as a reference, while the changes of T2 and T2 * values were consistent with MR images. The signal intensity is generally affected by several factors, such as magnetic field, pulse uniformity, repetition time (TR), and time to echo (TE), while the relaxation time was relatively constant. Regions with low signal intensity were noted in T2WI, T2 mapping, and T2 * mapping sequences on transplanted tumors on the first day after the injection of PMSCs. Therefore, according to the results obtained in the present study, it can be concluded that the regions with low signal intensity observed in the MR images in the experimental group were USPIOs-labelled PMSCs. The T2 and T2 * values of these regions were notably lower than those in tumor tissues; with decrease of T2 * value, the signal value of the labelled cells reached the lowest on the 2nd day, while the signal value of the labelled cells gradually increased on the third day. On the 7th day, the regions with low signal value were narrowed, and these areas in some tumors showed poor clarity. On the 10th day, the signal value of the tumor tissue increased. On the 14th day, there was no significant difference between the experimental group and the control group, and a large area of necrosis could be observed in the tumor.

For T2 mapping and T2 * mapping sequences in the experimental group, the TE value increased, the SNR decreased, and the CNR value slightly increased. The longer the TE is, the worse the SNR of the image is, while the CNR of the image is superior. Therefore, selection of an appropriate TE is particularly important for medical imaging. Several [19, 20]scholars demonstrated that the T2 * mapping sequence was not significantly different from T2 mapping in the imaging and quantification of iron in the tissue. In the current study, it was unveiled that the T2 * value of the labelled cells in the experimental group was lower than the T2 value. Comparing the image quality of T2WI, T2 mapping, and T2 * mapping sequences on USPIOs-labelled PMSCs, we that found the SNR of T2 * mapping image was not significantly different from T2 mapping, in which both were higher than T2WI sequence. T2 * mapping sequences of labelled cells and tumor tissues were more obvious than T2WI and T2 mapping sequences, indicating that T2 * mapping sequences are superior to T2WI and T2 mapping sequences in the study of USPIOs-labelled PMSCs.

A number of scholars reported that MSCs can recruit lymphocytes for cancerous tissues, inhibit cell proliferation, and promote cell apoptosis. However, in the present experiment, HE staining of USPIOs-labelled PMSCs revealed that the MVD of cancer cells did not significantly increase or decrease, the necrotic area around the cancer tissue gradually increased over time, and the degree of malignancy was extremely high. Regions with low signal intensity were found in the MR images in the experimental group, Perls' Prussian blue staining after scanning on day 1 confirmed the presence of USPIOs-labelled PMSCs; on day 14, no obvious Prussian blue-stained particles were found in the tumors in the experimental group and the control group, indicating that PMSCs were metabolized. Additionally, in the current research, CD31 and CD34 were highly expressed in vascular endothelium, and there were abundant new capillaries in the tumor; besides, there was no significant difference in the range and number of tumor blood vessels between the experimental group and the control group. Ki-67 has been widely applied as a striking potent biomarker in different medical-based researches. Furthermore, it was applied in researches on human subjects or animal models, malignancies behavior, aging and regenerative process. According to the various investigations, this biomarker can accurately signify the extent and percentage of proliferating cells in various malignancies, including renal cell carcinoma, adenocarcinoma, non-small cell lung cancer, soft tissue sarcoma, etc. [21, 22]. In the current research, Ki-67 was positively in both the experimental group and the control group, and the ratio of nucleus to cytoplasm was high, in which the increase and decrease of intracellular and extracellular space revealed the role of cancer cell proliferation, while the injection of PMSCs did not significantly affect the proliferation of CRC cells.

The current experiment confirmed that the USPIOs-labelled PMSCs had high labeling efficiency, while cell viability, proliferation ability, and apoptotic rate were not markedly influenced. labelled cells injected into CRC transplanted tumors were studied for a long period of time, and only a certain inhibitory effect on growth of tumor volume was noted, while no meaningful influence on tumor proliferation and angiogenesis was found. In subsequent studies, it may be possible to increase the number of injected PMSCs or establish a less malignant xenograft tumor model to prolong the rate of tumor development, so as to further study the underlying mechanism of PMSCs inhibiting tumor growth rate. In addition, as the cell divides and proliferates, the intracellular iron content gradually decreases, causing the MRI signal to fall below the detectable threshold, affecting the long-term observation of magnetized labelled cells. How to effectively combine MRI tracer signal with USPIO change in tissue remains to be further studied.

Conclusion

1. Ultrasmall superparamagnetic iron oxides(USPIOs) can effectively labelled human placental mesenchymal stem cells(PMSCs) at a certain concentration, while cell viability, proliferation ability, and apoptotic rate were not markedly influenced .
2. Magnetic labelled cells injected into CRC transplanted tumors can study for a long period of time, 3.0 T MRI in vivo molecular imaging is feasible.
3. PMSCs has a certain inhibitory effect on growth of colorectal tumor volume, while no meaningful influence on tumor proliferation and angiogenesis was found, the underlying mechanism remains to

be further studied.

Abbreviation

CRC colorectal cancer

PMSCs placental mesenchymal stem cells

USPIOs ultrasmall superparamagnetic iron oxides

PLL poly-L-lysine

ROI region of interes

MVD microvascular density

Declarations

Ethics approval and consent to participate

No human experiment is involved in the study, and the animal experiment has been approved by the ethics committee of the General Hospital of Ningxia Medical University.

Consent for publication

The author of the paper voluntarily transfers the right to assemble the paper (part or all of the paper), the right of reproduction, network communication and the printed and electronic versions to the editorial department has obtained the consent of all the authors.

Availability of data and material

All methods were carried out in accordance with relevant guidelines and regulations. All the data and materials in this study are true and credible, without fraud and plagiarism. The content of this paper has not been published formally, and does not involve issues such as submitting one draft and two submissions.

Competing interests

The authors declare that there is no conflict of interest with any financial organization or corporation or individual that can inappropriately influence this work.

Funding

This study was funded by the National Natural Science Foundation of China;

Author' contributions

The corresponding author Yu-lin GUO is mainly responsible for the experimental planning, Fang WANG and Yao XIONG responsible for major cell and animal experiments, Hua HE and Jie-ting HU are involved in the data analysis of the experiment. All authors reviewed the manuscript.

Acknowledgements

Thanks to the Institute of Stem Cells of the General Hospital of Ningxia Medical University for the gift of placental mesenchymal stem cells.

References

1. Siegel R L, Miller K D, Jemal A. Cancer statistics, 2018[J]. CA: A Cancer Journal for Clinicians, 2018,68(1):7-30.
2. Bray F, Ferlay J, Soerjomataram I, et al. Global cancer statistics 2018: GLOBOCAN estimates of incidence and mortality worldwide for 36 cancers in 185 countries[J]. CA Cancer J Clin, 2018,68(6):394-424.
3. Vuik F E, Nieuwenburg S A, Bardou M, et al. Increasing incidence of colorectal cancer in young adults in Europe over the last 25 years[J]. Gut, 2019,68(10):1820-1826.
4. De Palma M, D B, TV P. Microenvironmental regulation of tumour angiogenesis.[J]. Nature reviews. Cancer, 2017,17(8):457-474.
5. B R, J F, V B, et al. Enzymes involved in tumor-driven angiogenesis: A valuable target for anticancer therapy.[J]. Seminars in cancer biology, 2019,56:87-99.
6. C V, B L. Tumor angiogenesis and vascular normalization: alternative therapeutic targets.[J]. Angiogenesis, 2017,20(4):409-426.
7. R R, M B, S M, et al. Tumor angiogenesis revisited: Regulators and clinical implications.[J]. Medicinal research reviews, 2017,37(6):1231-1274.
8. Mattar P, Bieback K. Comparing the Immunomodulatory Properties of Bone Marrow, Adipose Tissue, and Birth-Associated Tissue Mesenchymal Stromal Cells[J]. Front Immunol, 2015,6:560.
9. Oliveira M S, Barreto-Filho J B. Placental-derived stem cells: Culture, differentiation and challenges[J]. World J Stem Cells, 2015,7(4):769-775.
10. EG R, BL P, K H, et al. Evaluation of Placental Mesenchymal Stem Cell Sheets for Myocardial Repair and Regeneration.[J]. Tissue engineering. Part A, 2019,25(null):867-877.
11. Roberts E G, Piekarski B L, Huang K, et al. Evaluation of Placental Mesenchymal Stem Cell Sheets for Myocardial Repair and Regeneration[J]. Tissue Eng Part A, 2018.
12. C M, von der Ohe J, R H. MSC stimulate ovarian tumor growth during intercellular communication but reduce tumorigenicity after fusion with ovarian cancer cells.[J]. Cell communication and signaling : CCS, 2018,16(1):67.

13. SR B, T L, M P, et al. Blocking Tumor-Educated MSC Paracrine Activity Halts Osteosarcoma Progression.[J]. Clinical cancer research : an official journal of the American Association for Cancer Research, 2017,23(14):3721-3733.
14. C M, Y Y, R H. Interaction of MSC with tumor cells.[J]. Cell communication and signaling : CCS, 2016,14(1):20.
15. X Z, H Z, Z C, et al. Ultrasmall superparamagnetic iron oxide nanoparticles for magnetic resonance imaging contrast agent.[J]. Journal of nanoscience and nanotechnology, 2014,14(1):210-220.
16. Dadfar S M, Roemhild K, Drude N I, et al. Iron oxide nanoparticles: Diagnostic, therapeutic and theranostic applications[J]. Adv Drug Deliv Rev, 2019,138:302-325.
17. Q L, L S, S C, et al. A superparamagnetic polymersome with extremely high T relaxivity for MRI and cancer-targeted drug delivery.[J]. Biomaterials, 2017,114:23-33.
18. Dekkers I A, Lamb H J. Clinical application and technical considerations of T1 & T2(*) mapping in cardiac, liver, and renal imaging[J]. Br J Radiol, 2018,91(1092):20170825.
19. AS L, PD G, RH M. T2 mapping and T2* imaging in heart failure.[J]. Heart failure reviews, 2017,22(4):431-440.
20. G A, M W. T2* mapping of articular cartilage: current status of research and first clinical applications.[J]. Investigative radiology, 2014,49(1):57-62.
21. M J, Ľ D, Š P, et al. Ki67, PCNA, and MCM proteins: Markers of proliferation in the diagnosis of breast cancer.[J]. Acta histochemica, 2016,118(5):544-552.
22. LT L, G J, Q C, et al. Ki67 is a promising molecular target in the diagnosis of cancer (review).[J]. Molecular medicine reports, 2015,11(3):1566-1572.

Figures

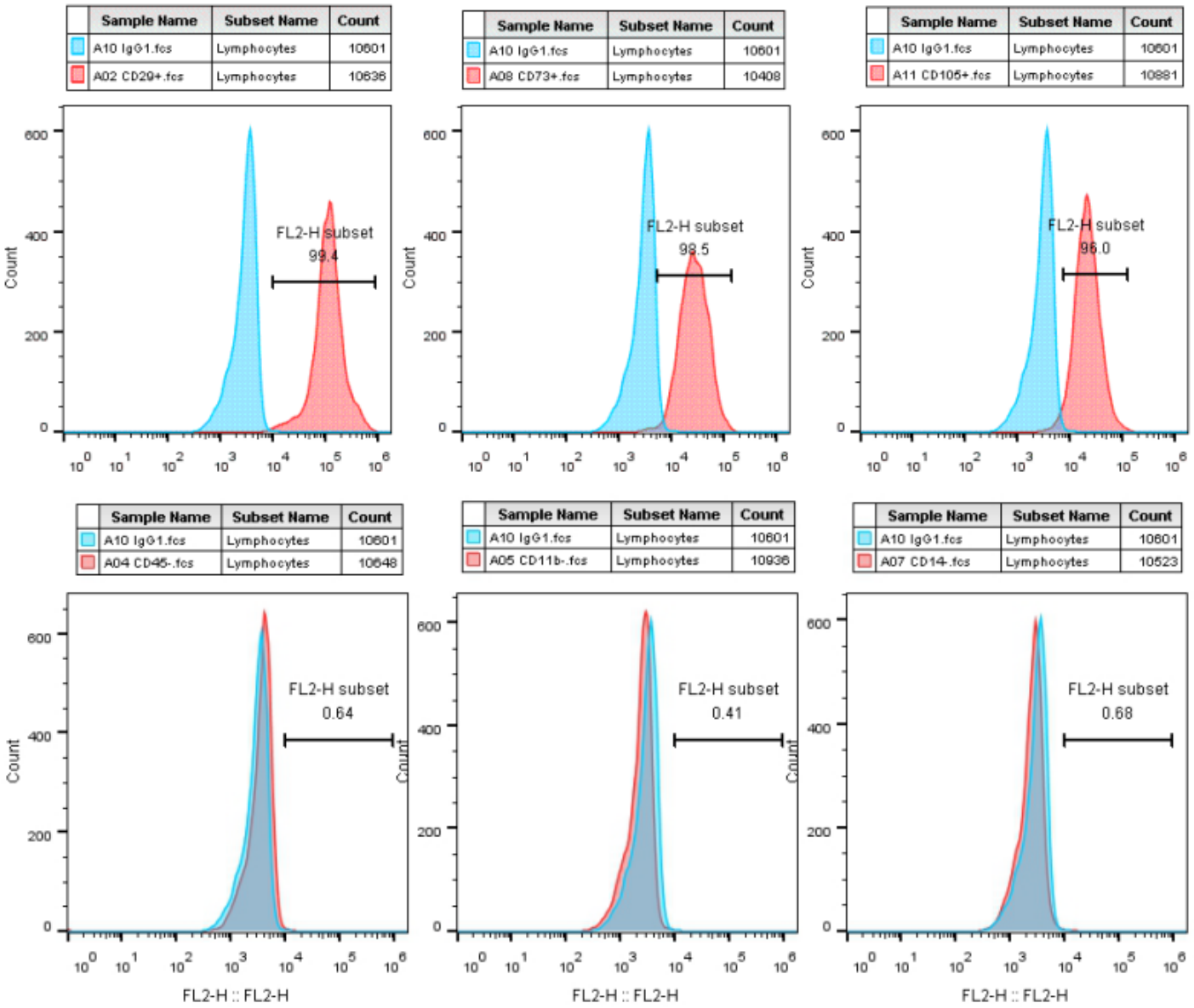

Figure 1

Identification of surface antigens in PMSCs

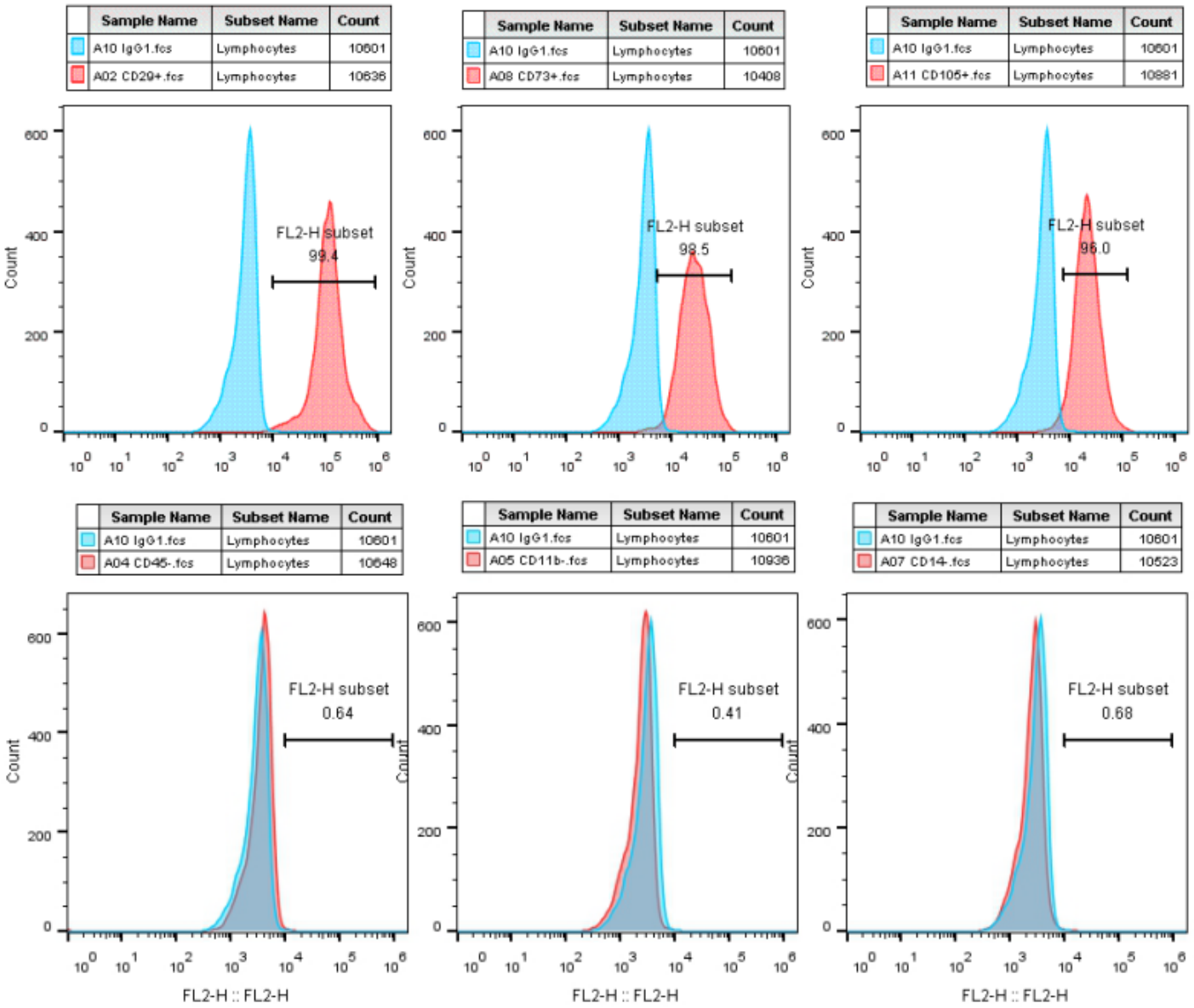

Figure 1

Identification of surface antigens in PMSCs

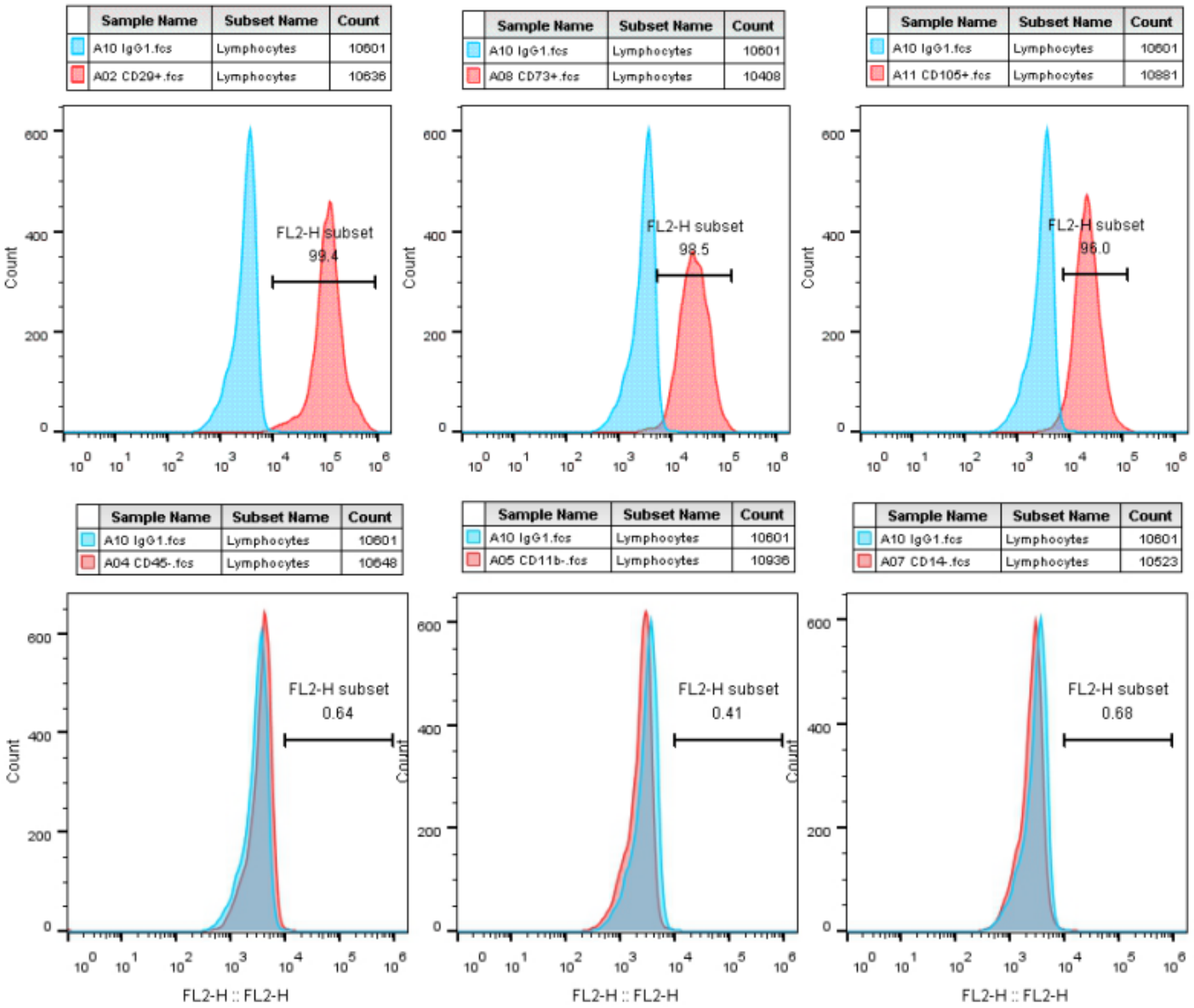

Figure 1

Identification of surface antigens in PMSCs

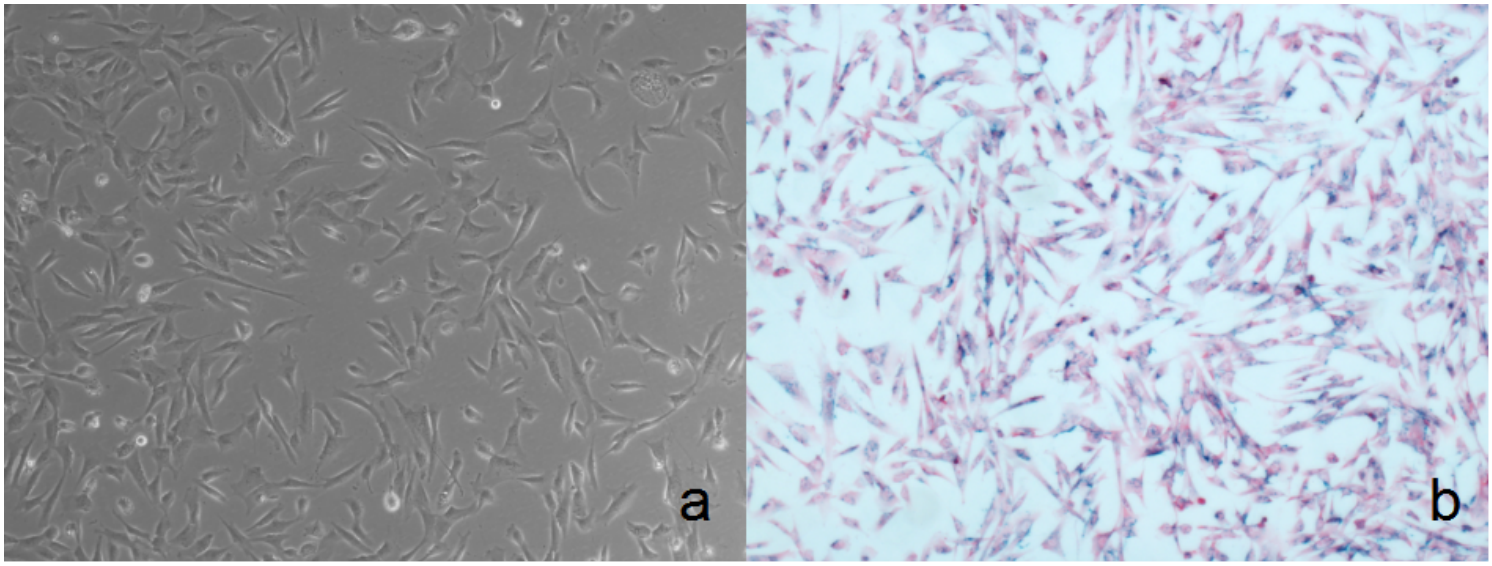

Figure 2

Prussian blue staining of magnetically labeled PMSCs (X100)

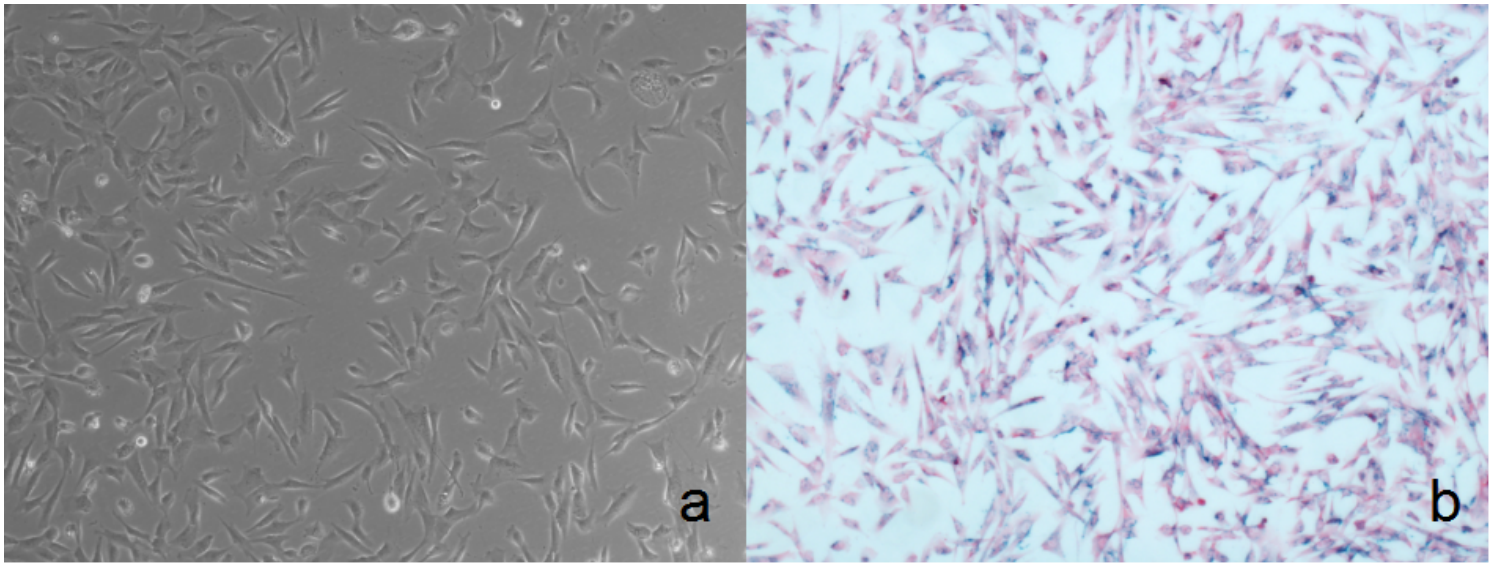

Figure 2

Prussian blue staining of magnetically labeled PMSCs (X100)

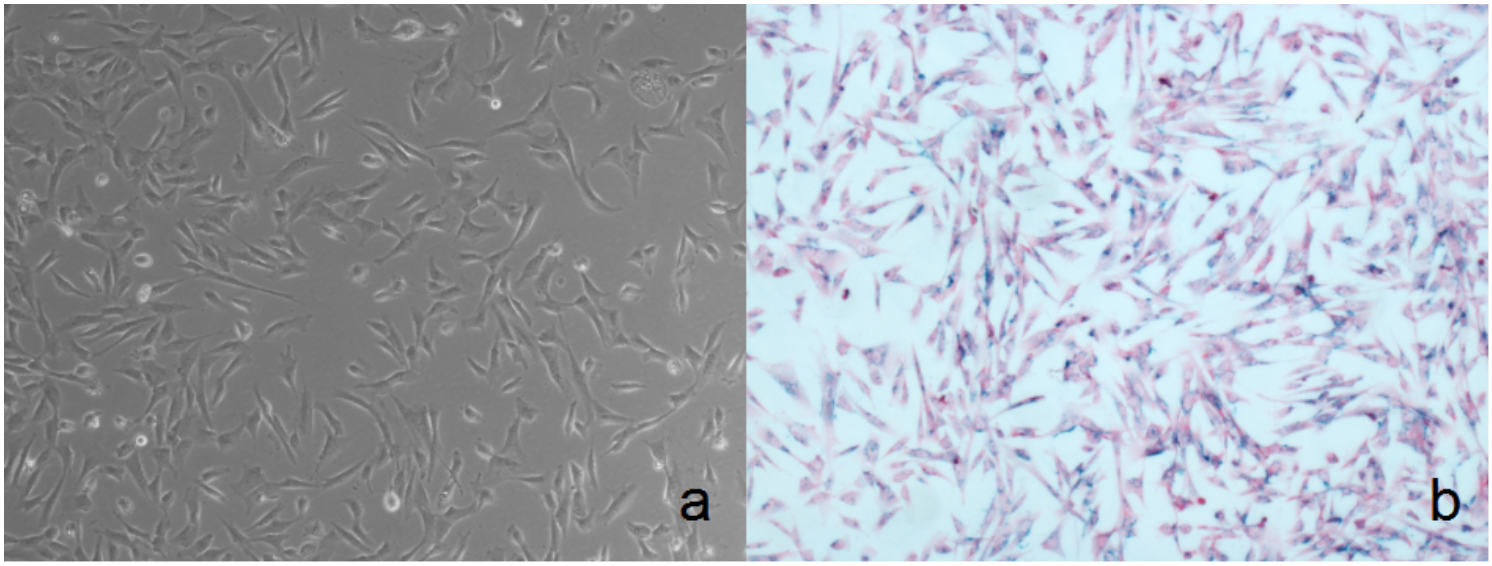

Figure 2

Prussian blue staining of magnetically labeled PMSCs (X100)

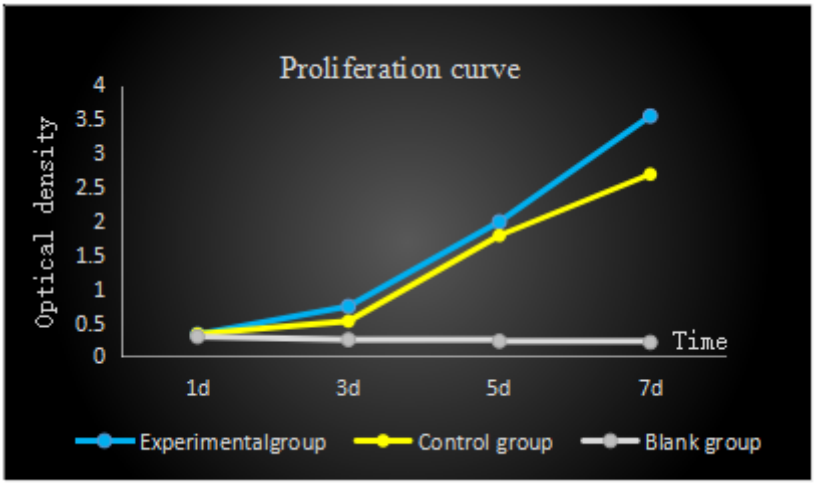

Figure 3

Comparison of MSCs proliferation ability between unlabelled group and labelled group

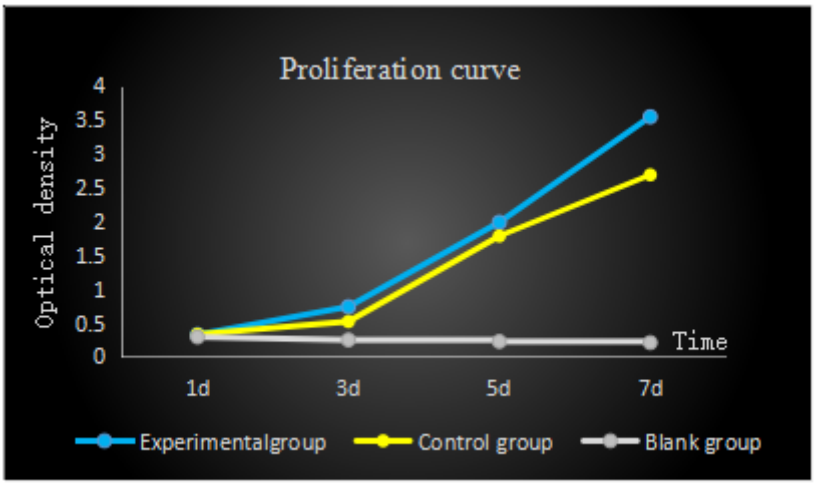

Figure 3

Comparison of MSCs proliferation ability between unlabelled group and labelled group

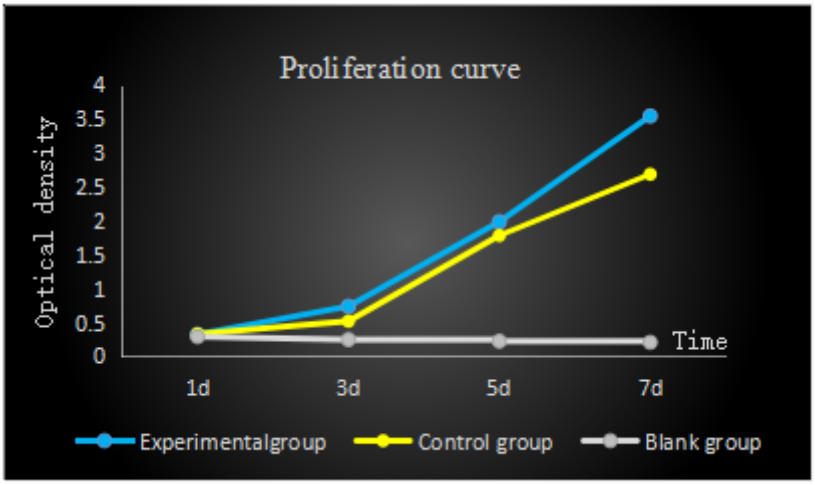

Figure 3

Comparison of MSCs proliferation ability between unlabelled group and labelled group

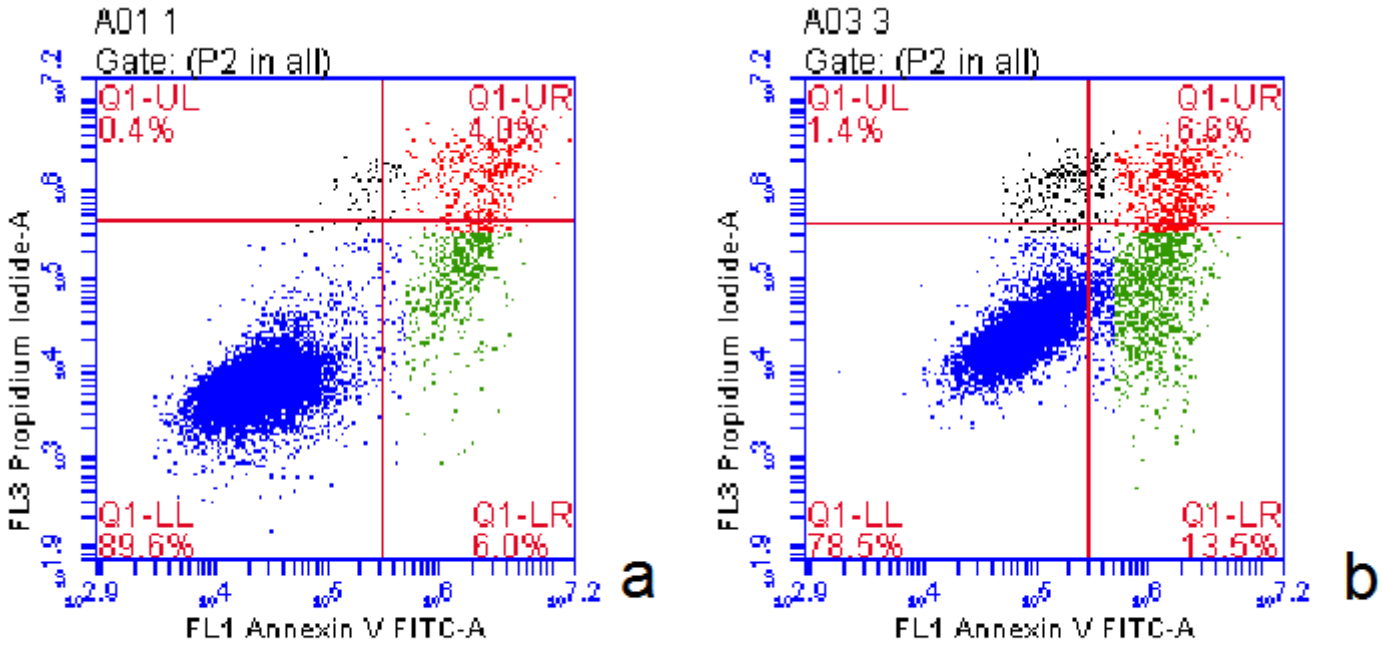

Figure 4

Unlabeled and labeled apoptosis rate compared (chart A showed unlabeled PMSCs apoptosis rate, chart B showed magnetically labeled PMSCs apoptosis rate)

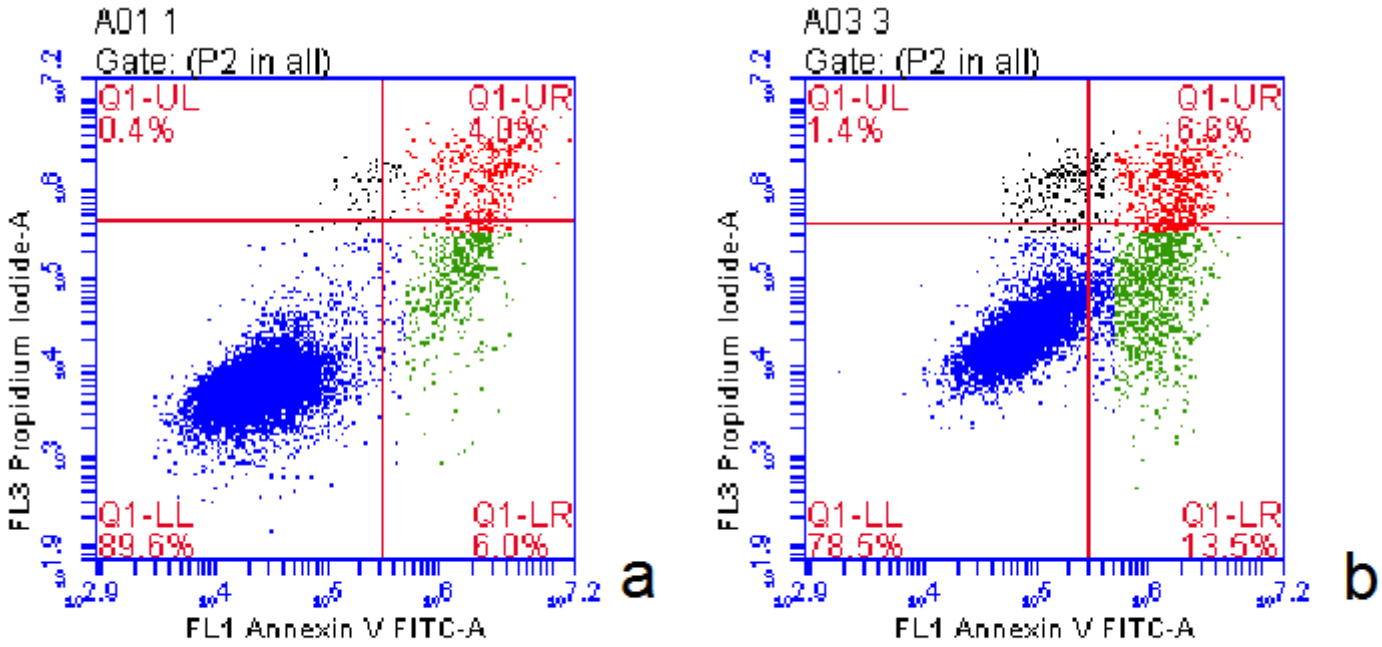

Figure 4

Unlabeled and labeled apoptosis rate compared (chart A showed unlabeled PMSCs apoptosis rate, chart B showed magnetically labeled PMSCs apoptosis rate)

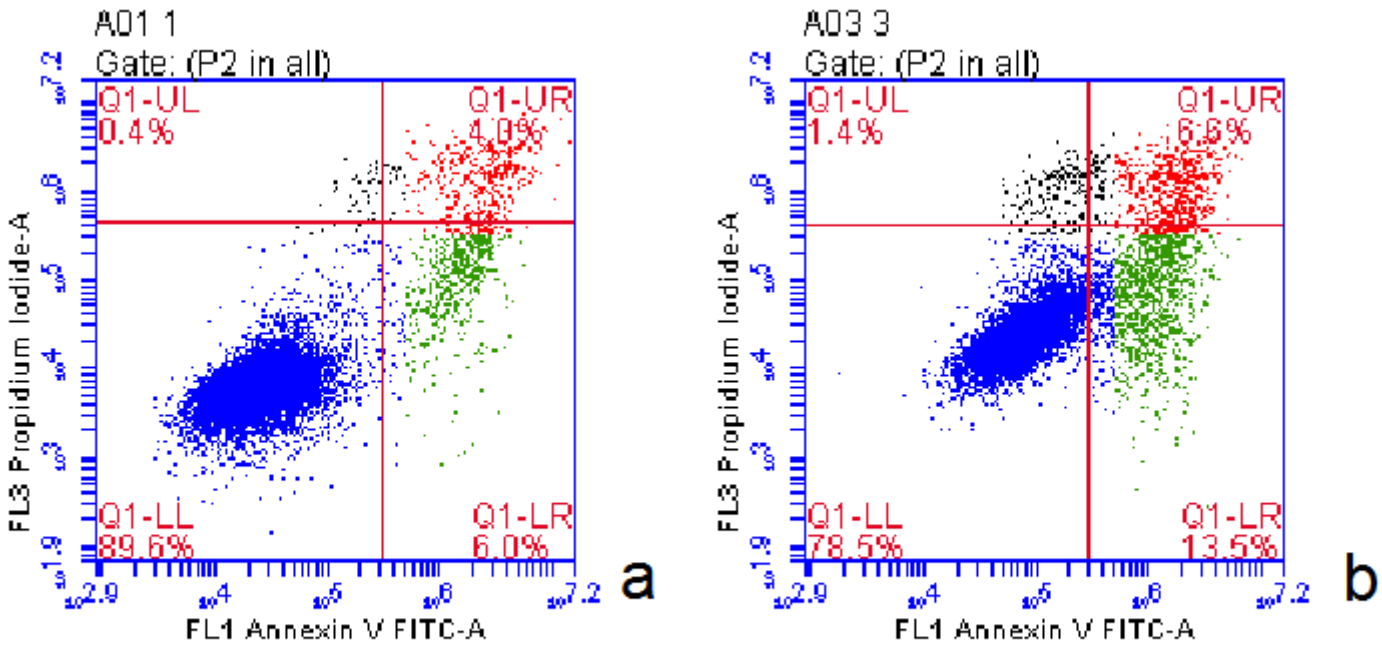

Figure 4

Unlabeled and labeled apoptosis rate compared (chart A showed unlabeled PMSCs apoptosis rate, chart B showed magnetically labeled PMSCs apoptosis rate)

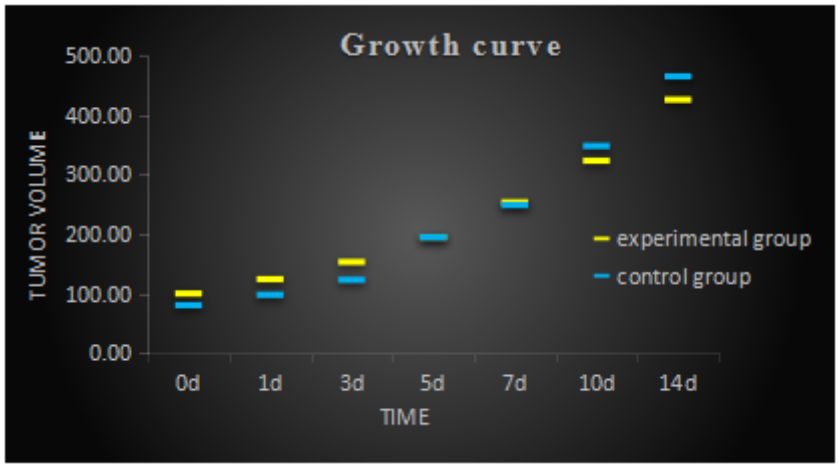

Figure 5

Comparison of growth curves between experimental and control group (n =8)

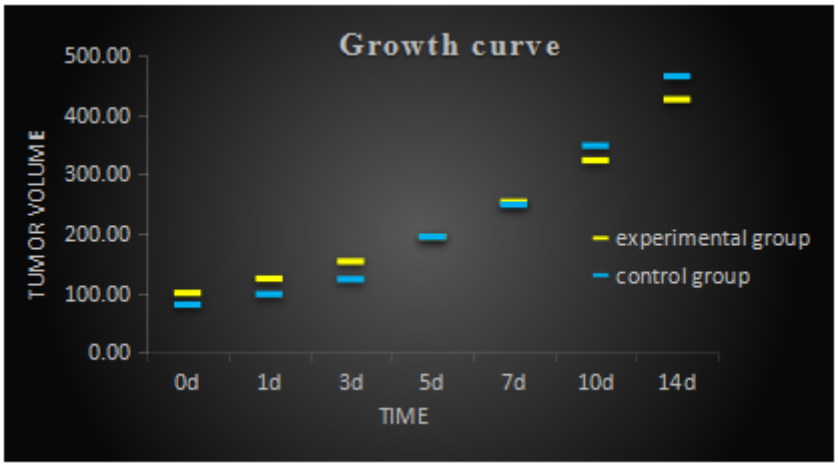

Figure 5

Comparison of growth curves between experimental and control group (n =8)

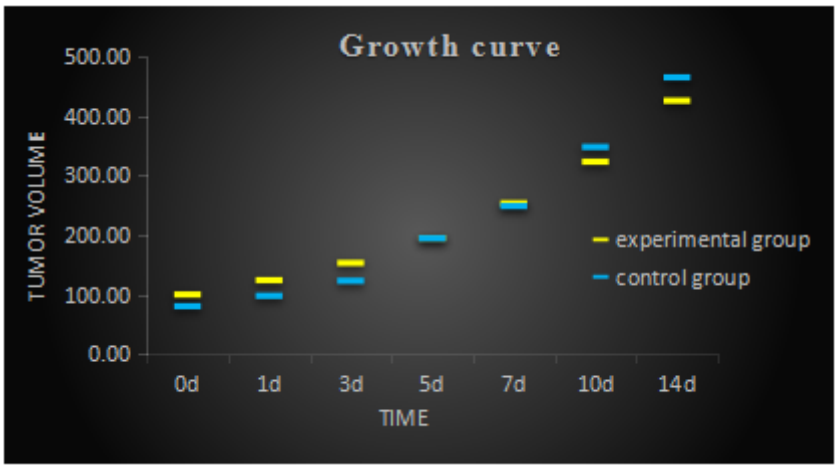

Figure 5

Comparison of growth curves between experimental and control group (n =8)

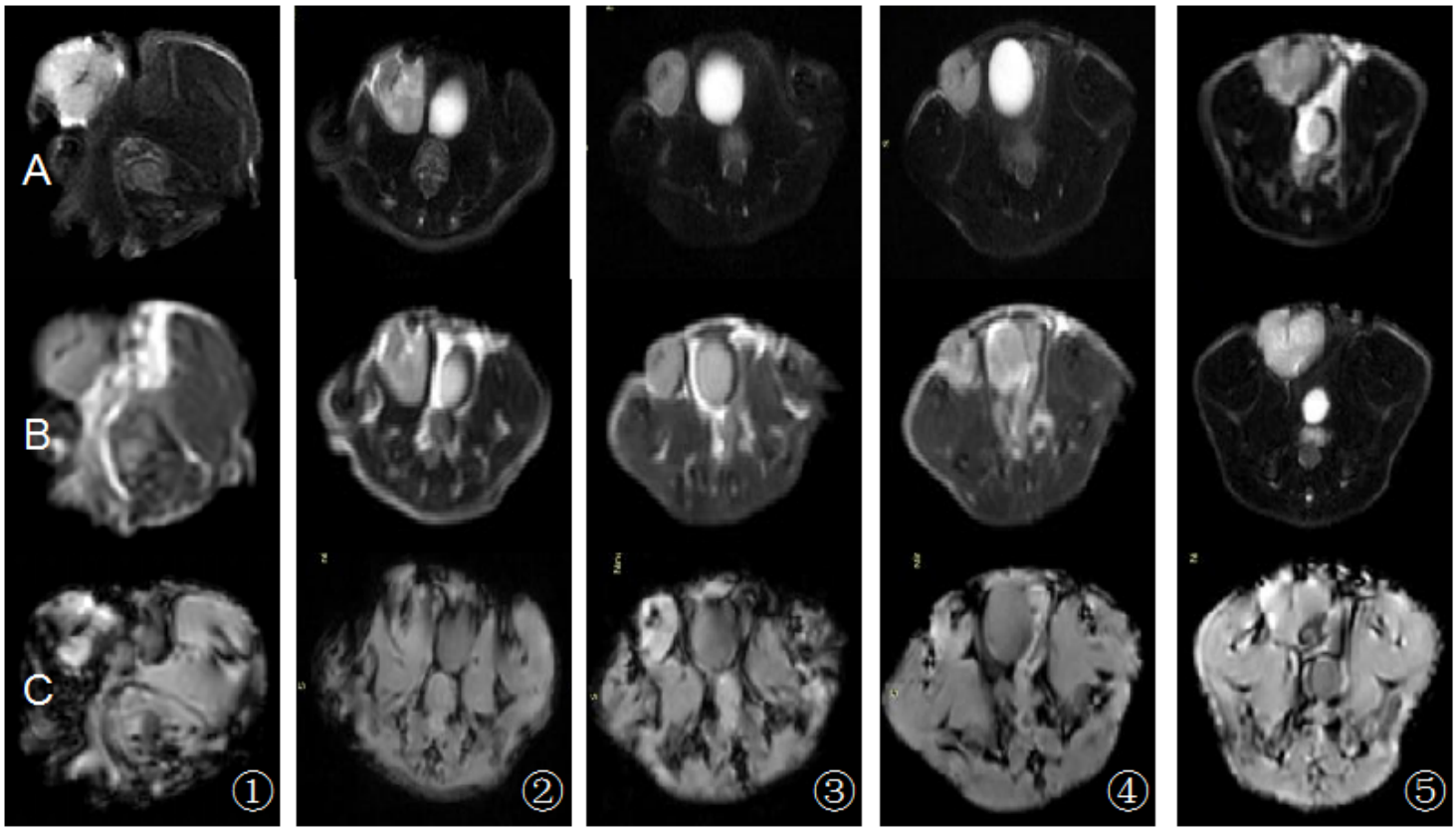

Figure 6

Different sequence imaging of transplanted mice (lines A, B and C were T2WI, T2mapping and T2*mapping images of experimental group, respectively, and 1-5 were MR images of experimental group for days 1,3,7,10,14, respectively)

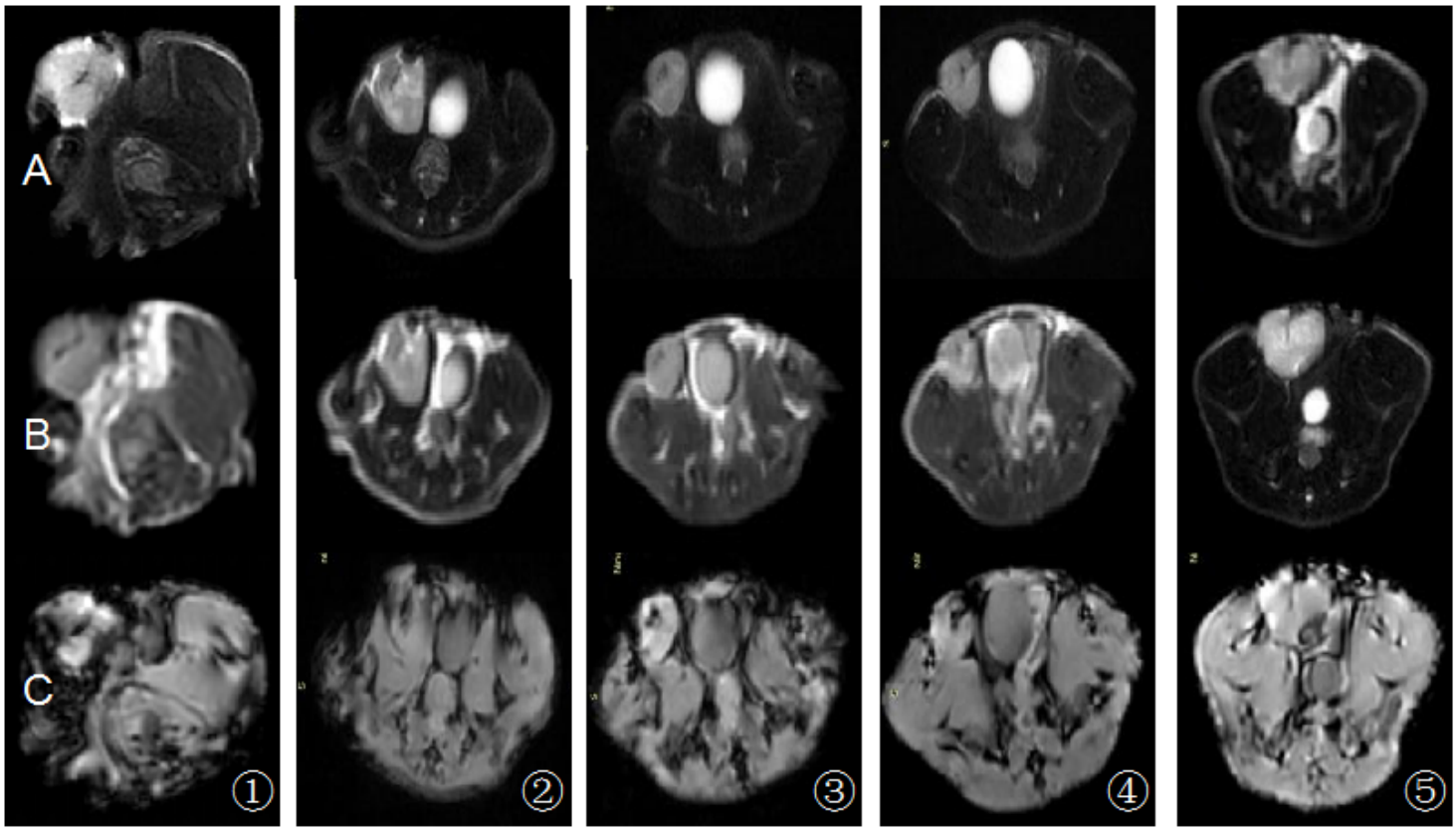

Figure 6

Different sequence imaging of transplanted mice (lines A, B and C were T2WI, T2mapping and T2*mapping images of experimental group, respectively, and 1-5 were MR images of experimental group for days 1,3,7,10,14, respectively)

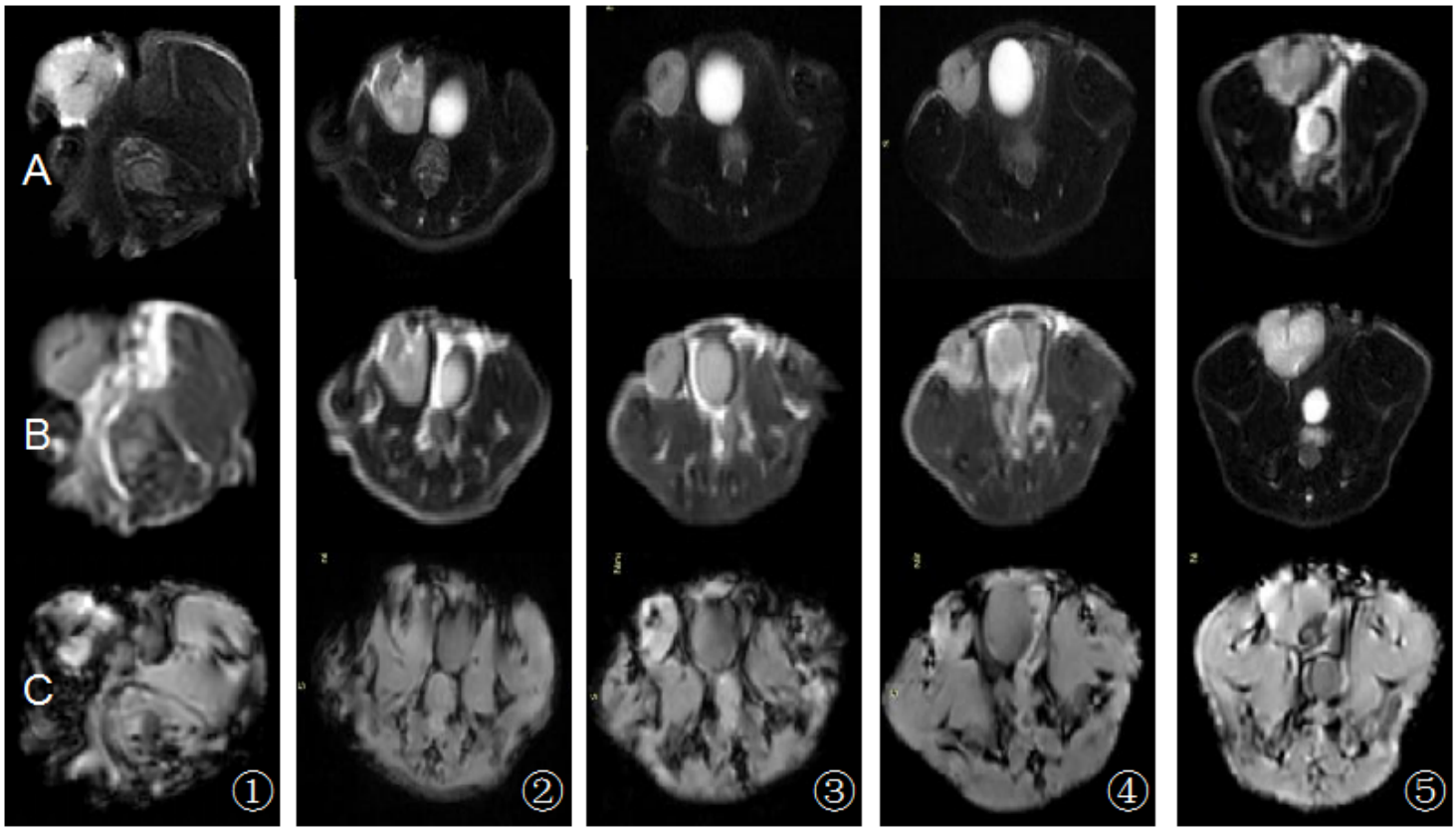

Figure 6

Different sequence imaging of transplanted mice (lines A, B and C were T2WI, T2mapping and T2*mapping images of experimental group, respectively, and 1-5 were MR images of experimental group for days 1,3,7,10,14, respectively)

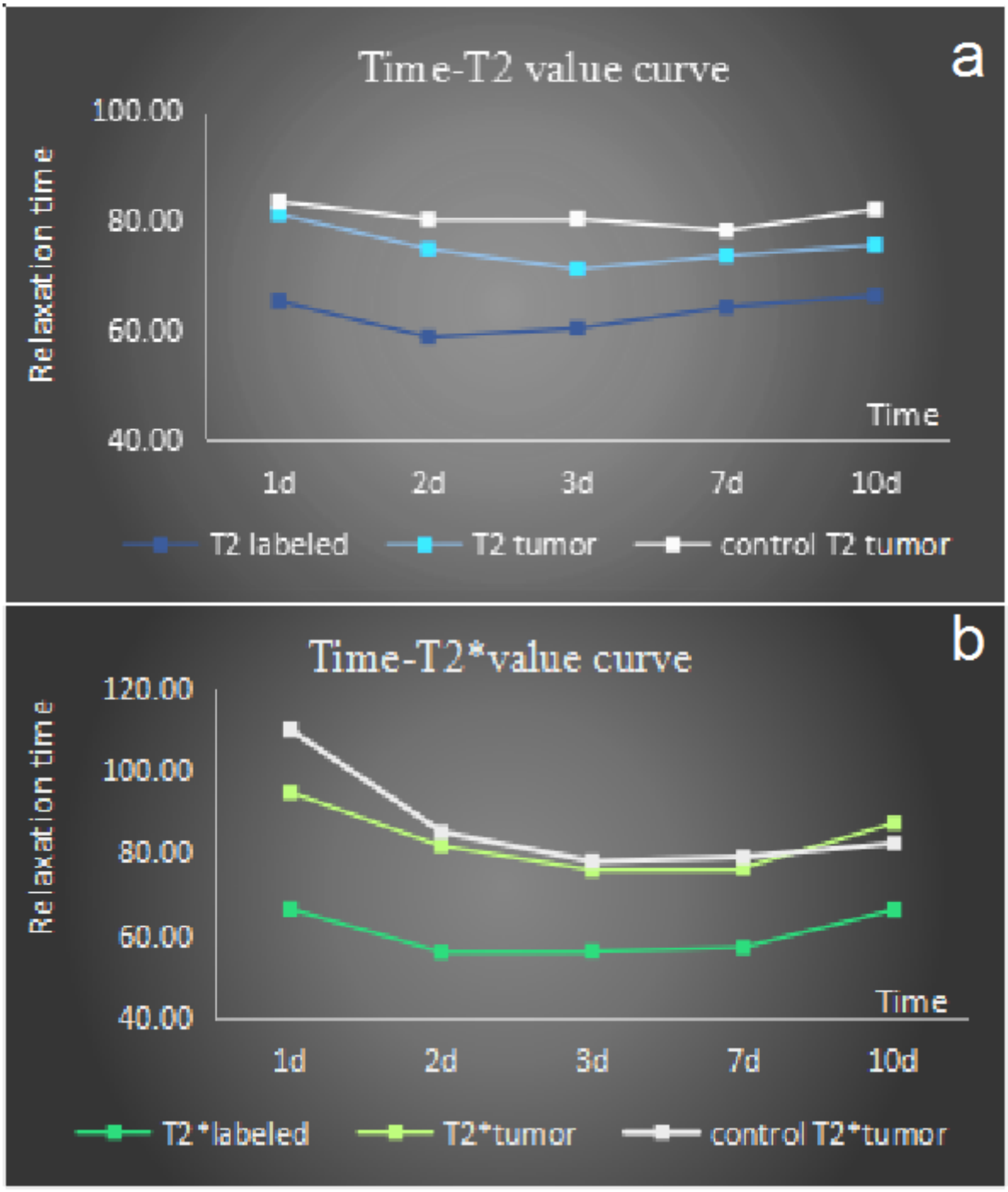

Figure 7

Time-signal value curve

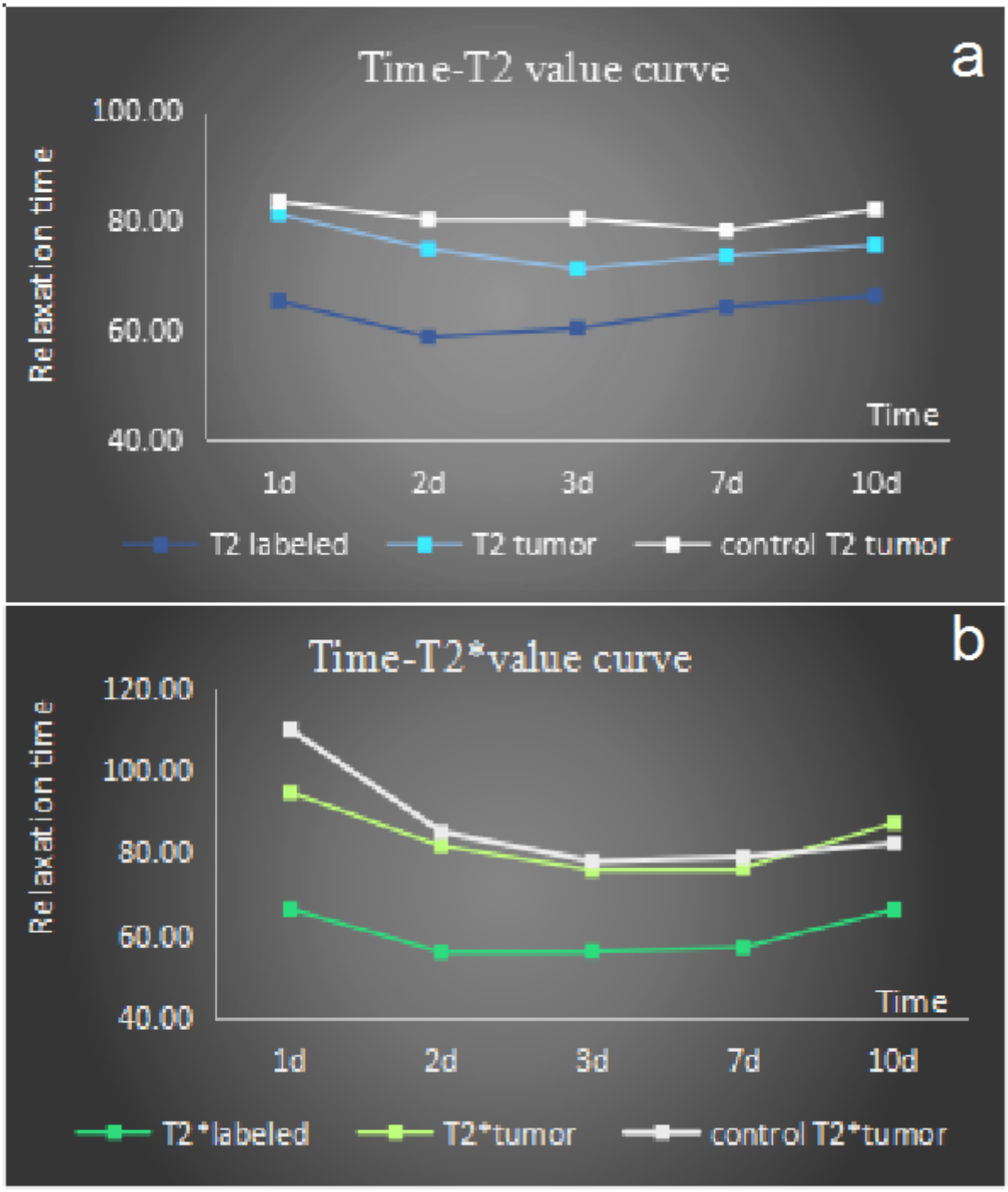

Figure 7

Time-signal value curve

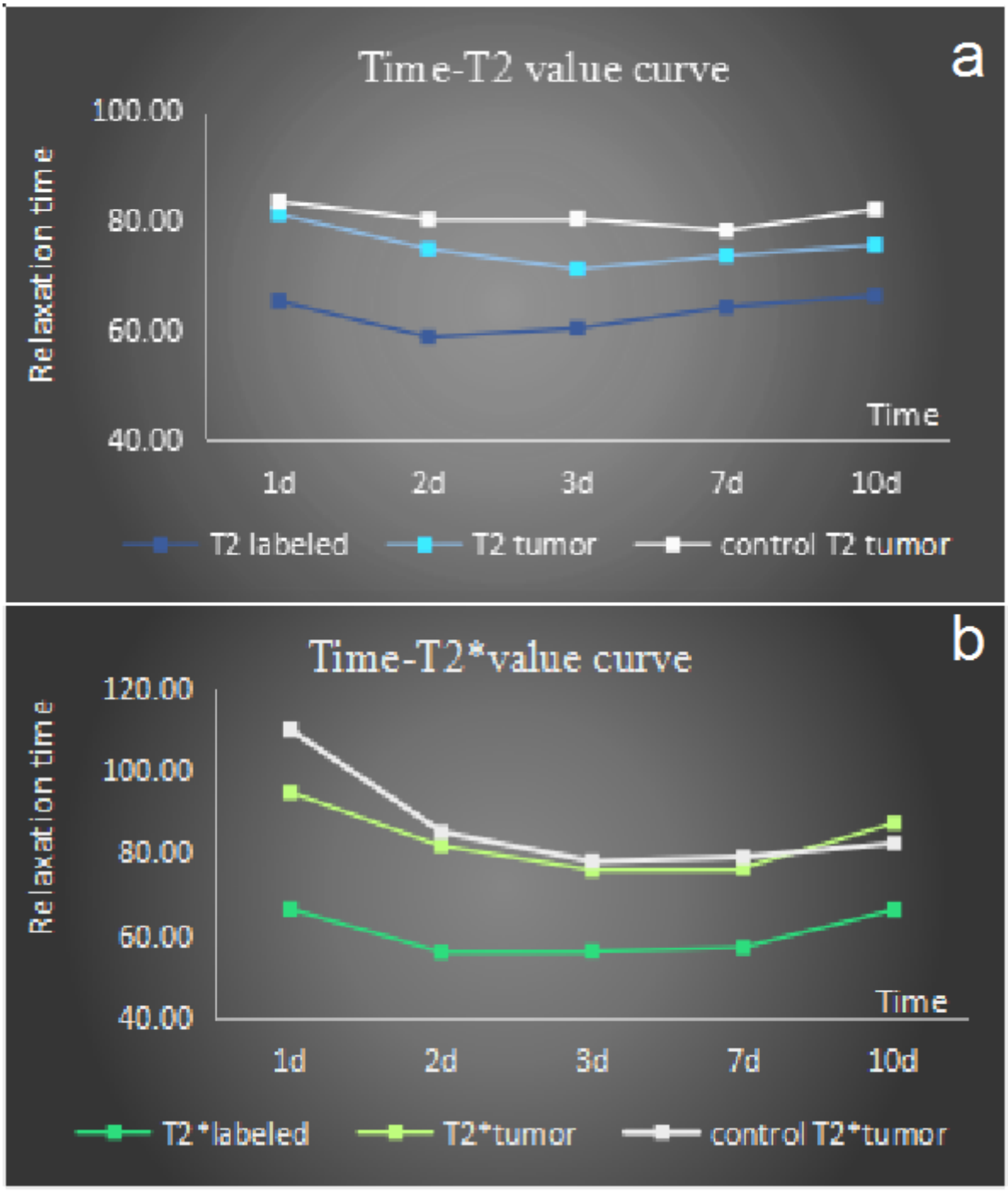

Figure 7

Time-signal value curve

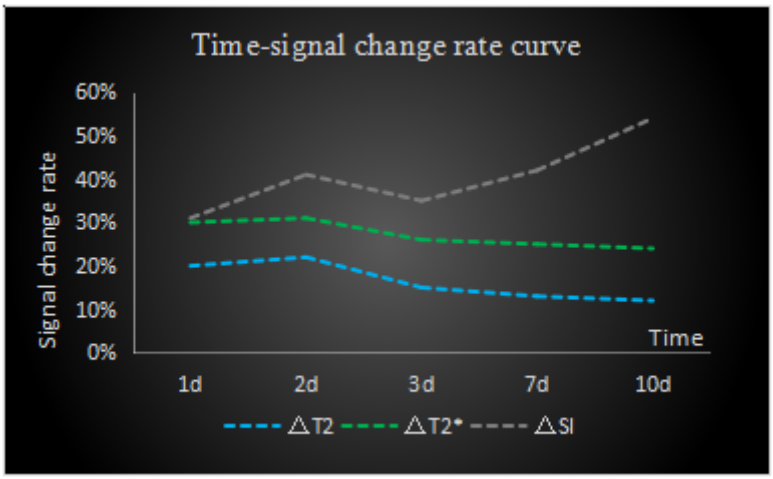

Figure 8

Time-signal change rate curve

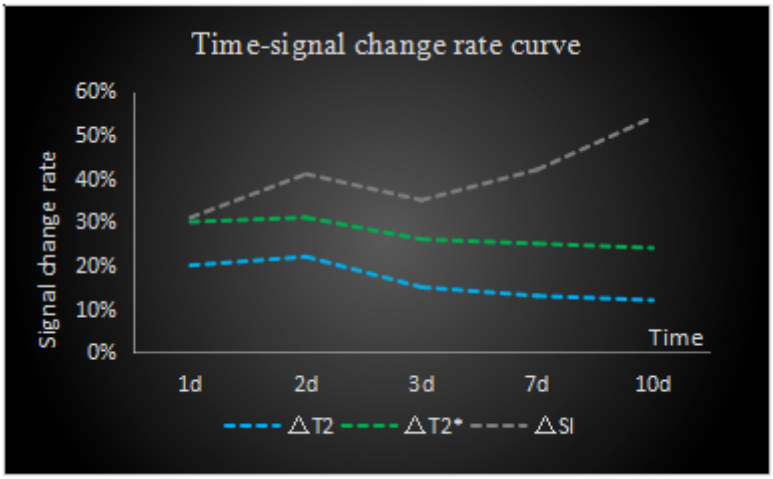

Figure 8

Time-signal change rate curve

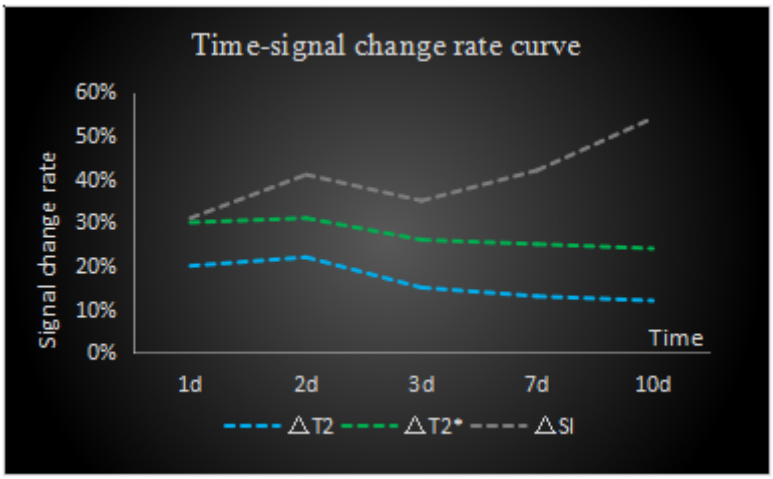

Figure 8

Time-signal change rate curve

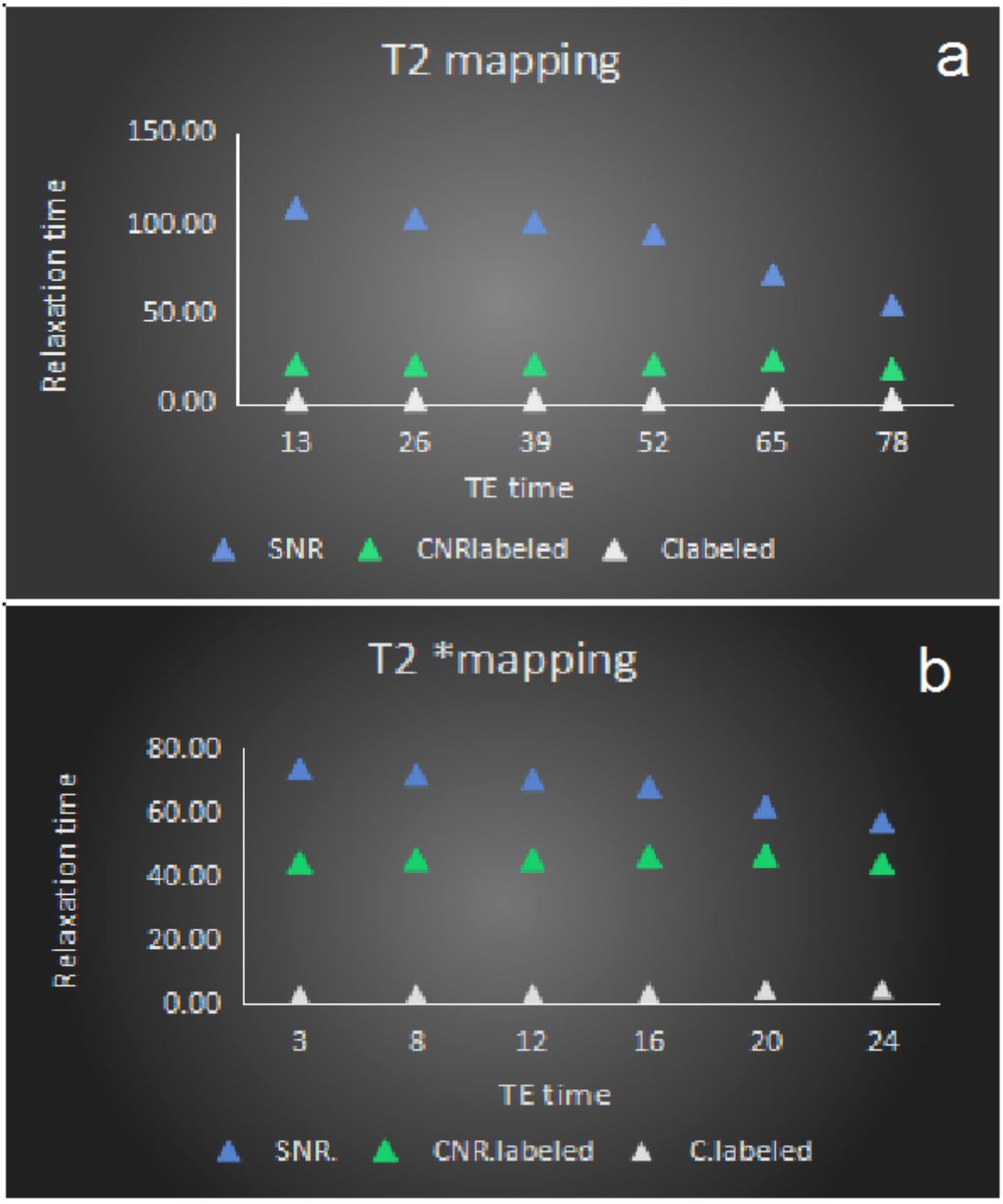

Figure 9

Comparison of Image Quality of Different TE Values

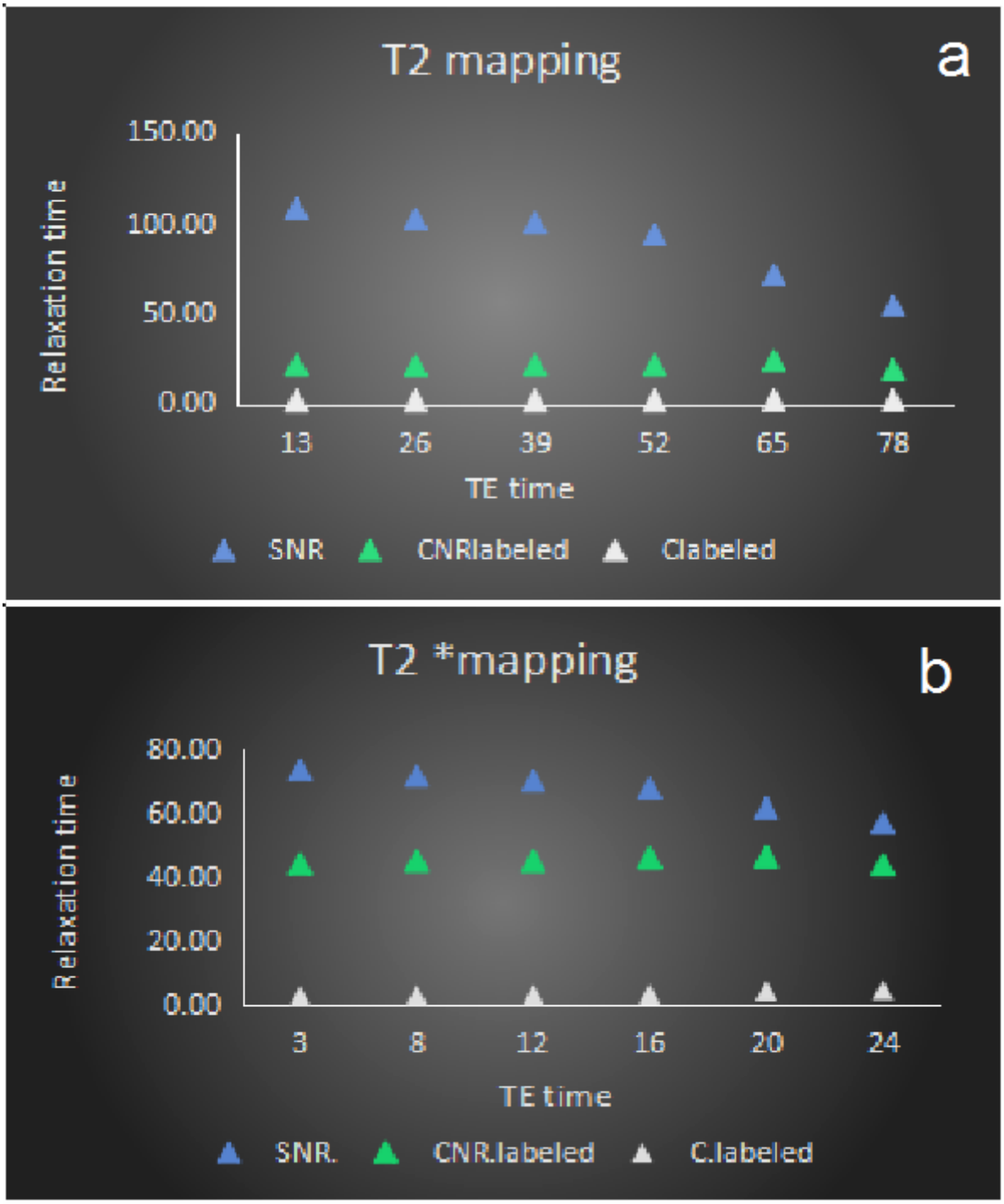

Figure 9

Comparison of Image Quality of Different TE Values

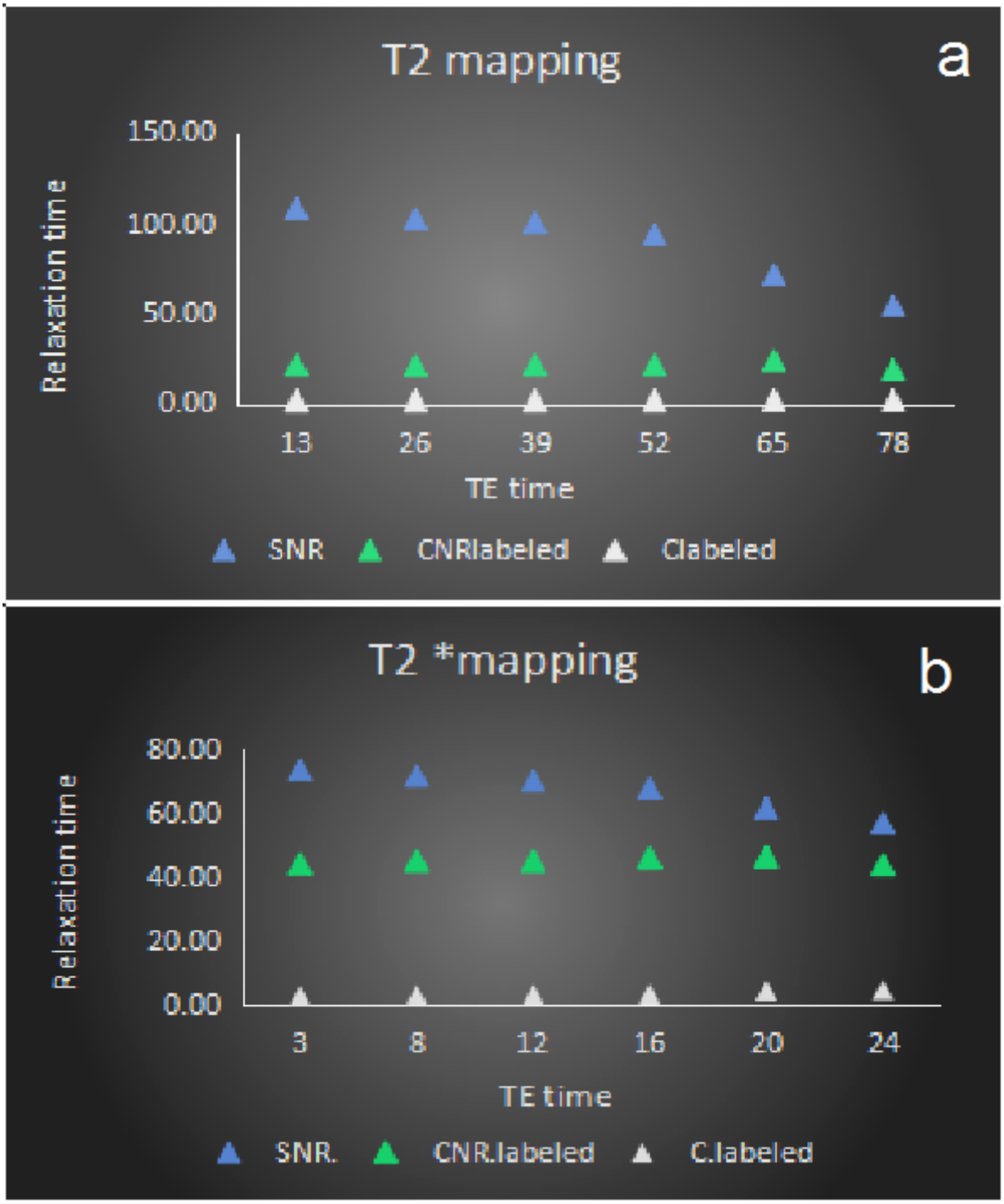

Figure 9

Comparison of Image Quality of Different TE Values

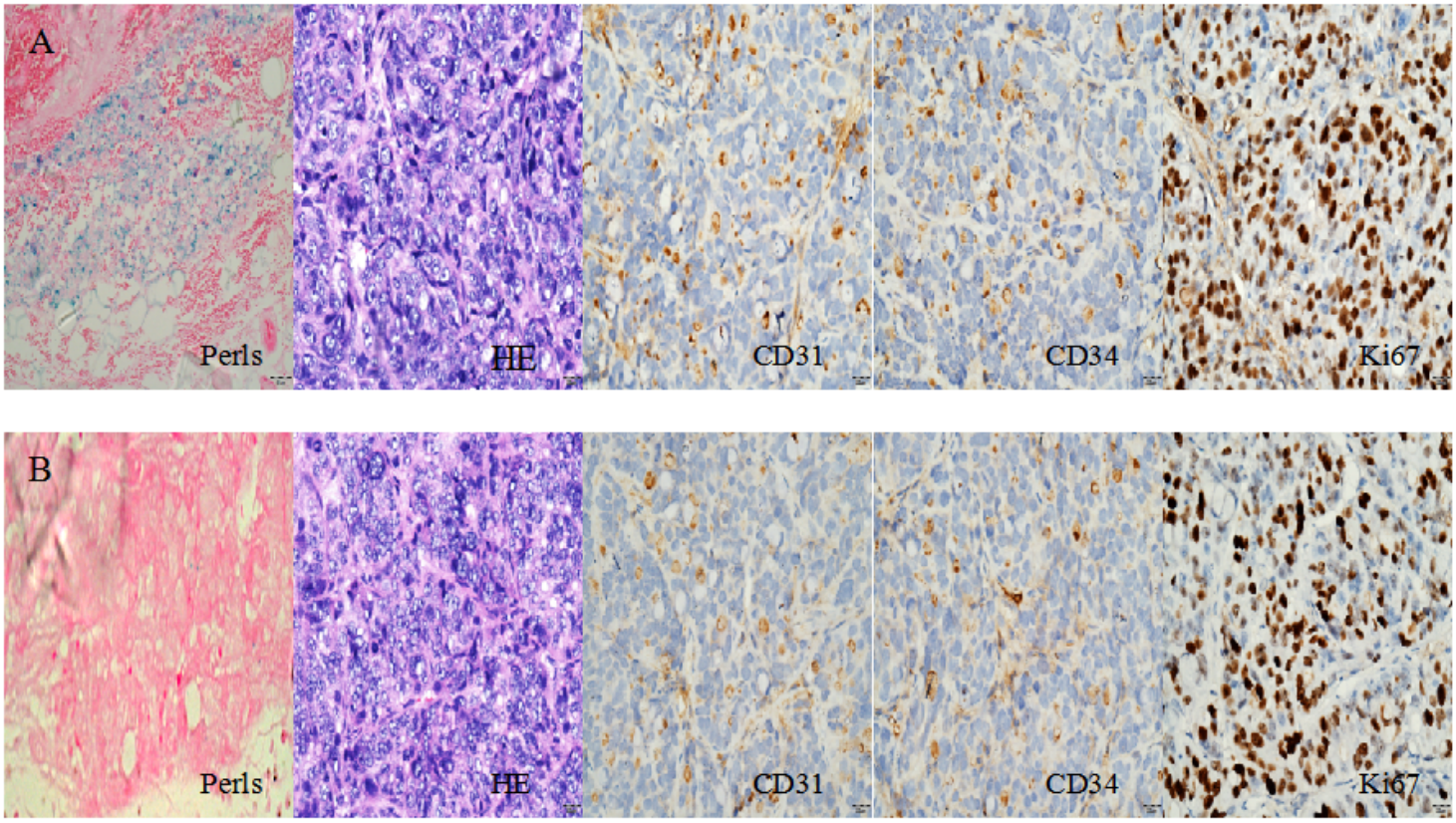

Figure 10

Results of pathological staining (line A and B were experimental group and control group, respectively)

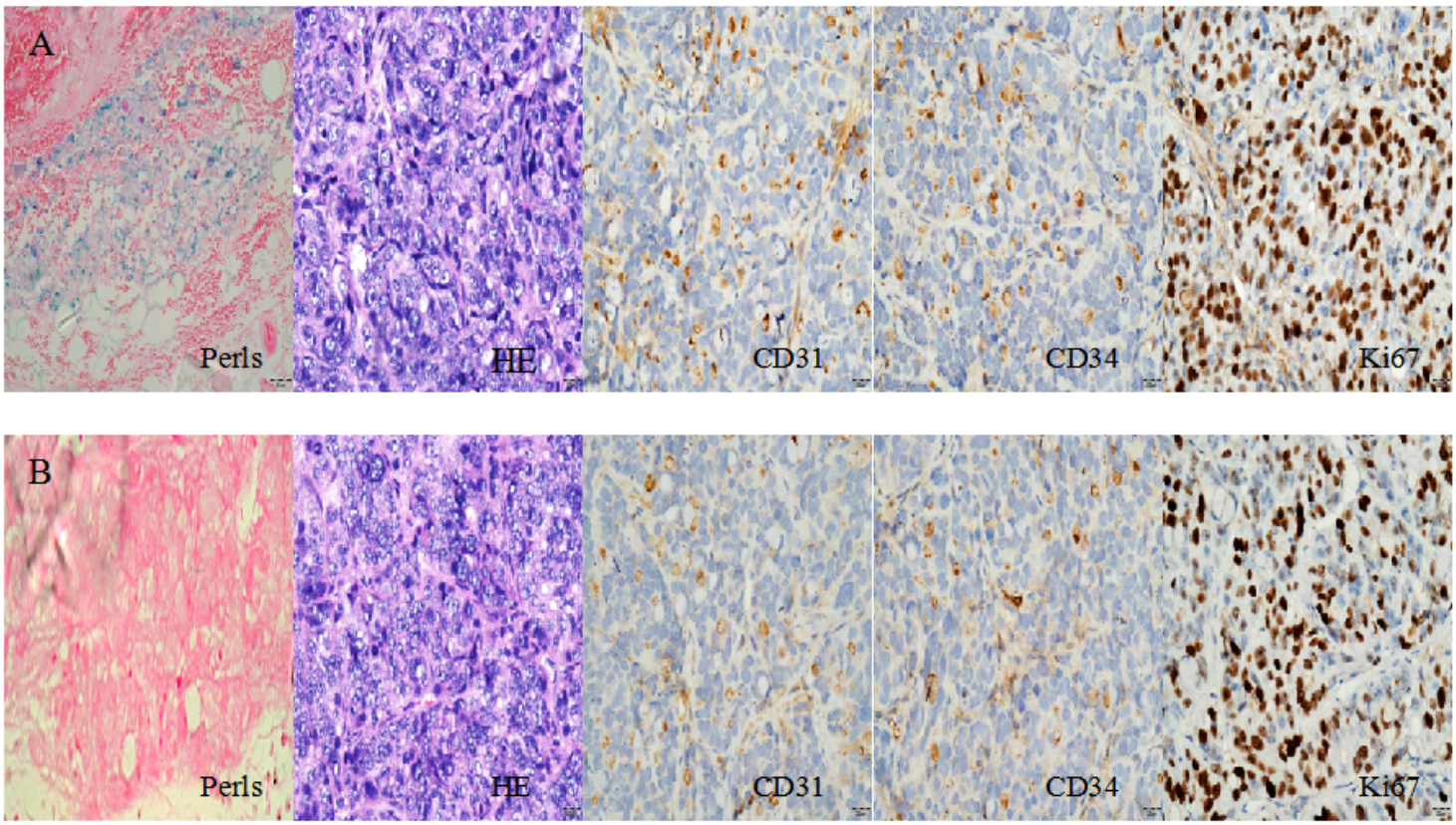

Figure 10

Results of pathological staining (line A and B were experimental group and control group, respectively)

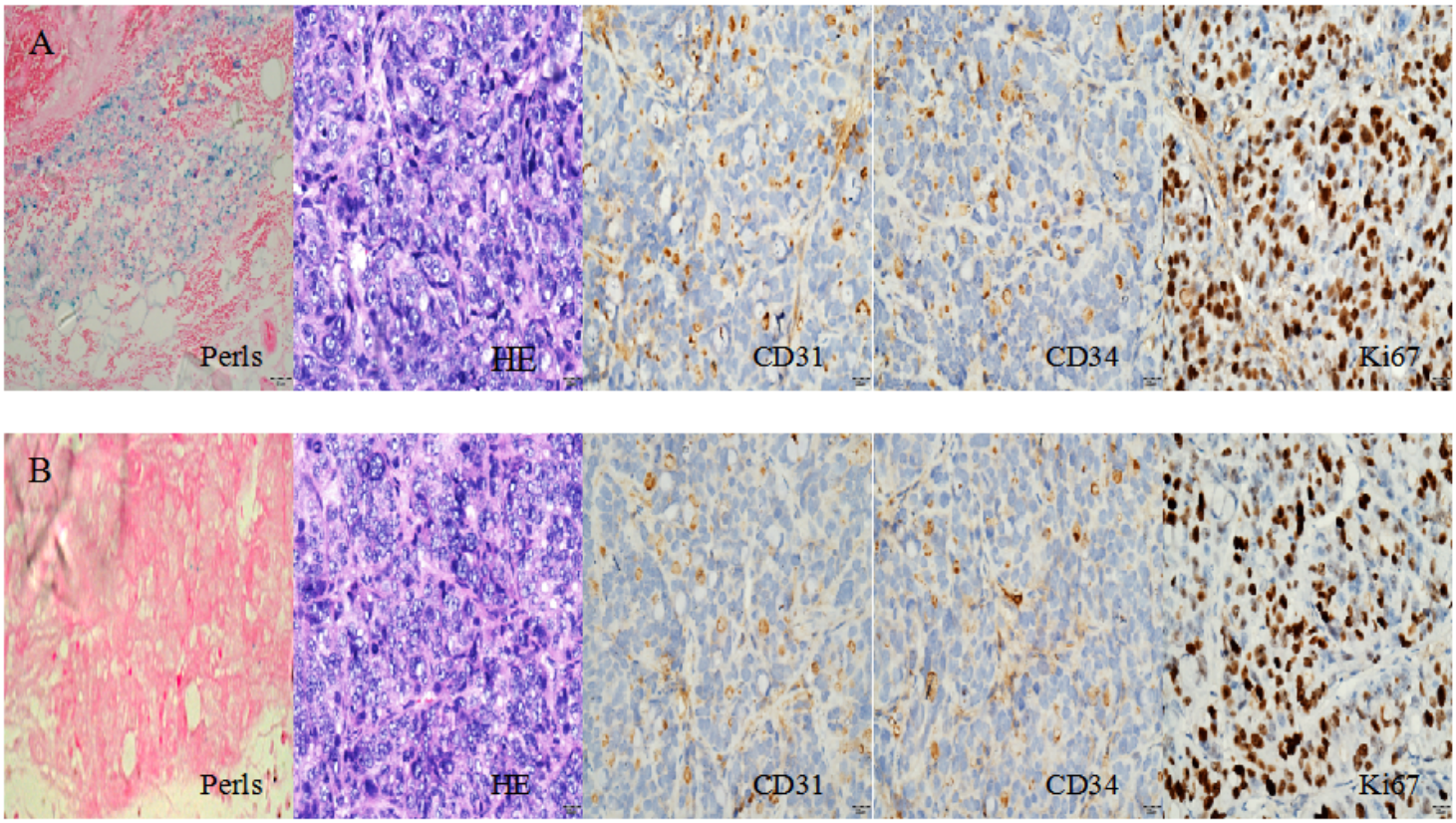

Figure 10

Results of pathological staining (line A and B were experimental group and control group, respectively)